J Solid State Electrochem (2011) 15:1811–1832
DOI 10.1007/s10008-011-1394-8

REVIEW

Free energy relationships in electrochemistry: a history that started in 1935

Anthony John Appleby · José Heráclito Zagal

Received: 27 January 2011 / Revised: 29 March 2011 / Accepted: 30 March 2011 / Published online: 31 May 2011

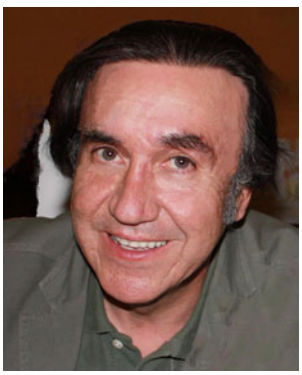

A. J. Appleby
Center for Electrochemical Systems and Hydrogen Research
3402, Texas A & M University,
College Station, TX 77843, USA

J. H. Zagal (✉)
Facultad de Química y Biología, Departamento de Química de los Materiales, Universidad de Santiago de Chile,
Casilla 40, Sucursal Matucana,
Santiago 9170022, Chile
e-mail: jose.zagal@usach.cl

Abstract This article is a historical overview of free energy relationships in electrochemistry with the purpose of giving the reader an integrated view on how these correlations are interconnected in various aspects starting with free energy correlations for outer-sphere and inner-sphere processes, Tafel correlations, the Butler–Volmer equation, and electron transfer theories. The citation of the literature is far from complete and is aimed to stimulate the reader to further reading.

Keywords Tafel slopes · Butler–Volmer · Brønsted slopes · Marcus · Hush · Levich–Dogonadze · Volcano correlations

Introduction

The prediction of the rate of chemical reactions is a fundamental challenge in all areas of chemistry and biochemistry, and electrochemistry is not an exception. On the other hand, linear free energy correlations in the kinetics of families of similar chemical reactions are well known and essentially state that a linear correlation between the logarithm of the rate constant log k and the free energy of the reaction should be observed, implying that a linear correlation exists between the free energy of activation and the Gibbs free energy of the reaction for a given family of reactions (Brønsted plots). The slope of these correlations is a measure of the sensitivity of rate constant to structural changes in a family of reactions (analogous to the definition of ρ in Hammett plots in organic systems). Frumkin stated in 1932 [1] that, at different potentials, an electrode reaction can be considered as a series of similar reactions differing only by the value of $\Delta G°$, where $\Delta G°$ is equal to $-F\Delta E°$ [2], so in this case the role of substituents for changing the driving

force is played by the potential of the electrode applied by an external source. As discussed further down, these correlations are not always linear in electron transfer processes in the homogeneous phase or at electrode interfaces. In this article, we present a historical, not necessarily complete, overview of free energy relationships in electrochemistry with the purpose of giving the reader an integrated view on how these correlations are interconnected in various aspects starting with free energy correlations for outer-sphere and inner-sphere processes, Tafel correlations, the Butler–Volmer equation, and a discussion on different charge transfer theories.

Kinetic of charge transfer processes

These involve the transfer of charge to or from electrode reservoirs to reacting ions, atoms, or molecules. They are traditionally characterized by Tafel plots, which are plots of the logarithm of an electrochemical reaction rate (usually the rate expressed as an electrical current) versus the applied electrical potential, with respect to a reference electrode or to the reversible potential of the reaction in question. On the latter scale, this potential difference is known as the reaction overpotential, η. In some cases, the relationships have been documented as curves rather than straight lines. This is particularly so for the dioxygen reduction reaction (ORR) on various metal *hkl* surfaces in acid media [3–8]. Other authors have rationalized such curves as being the transition between two straight line plots with different slopes, reflecting either a change in reaction mechanism with overpotential or an effect due to changing the coverage of adsorbed species accompanied by a change in free energy of adsorption affecting the reaction rate [9].

Before discussing other interpretations of electrochemical kinetic reaction rates, it is appropriate to discuss the implications of relationships of Tafel type (with a further discussion of Tafel correlations to be given later). If we take a conventional view of chemical kinetics, which involve reactions between atoms and/or molecules, the addition of such low-mass particles or waves as electrons to their dynamics should not make much difference. A further reasoning behind this is that, in any case, electron transfers between atoms or molecules are involved in bond formation in conventional chemical processes. In 1926 [10], new forms of quantum mechanics made classical chemical kinetics a thing of the past in electrochemistry. Although Butler [2] maintained his thermodynamic-type approach until the mid-1930s, he realized that Gurney [11] had overtaken him. Many scientists were slow to follow Gurney [11]. Until the publication of the first paper of Nobel laureate Rudolph A. Marcus [12] in 1956, the kinetics of electrochemical reactions were regarded as a simple sub-set of chemical kinetic reactions, in which electrons from the equilibrium energy level of a metal electrode (its Fermi energy) happened to be reactants in a radiationless transfer process. This is clear in the first theoretical treatment of the hydrogen evolution reaction by Gurney in 1931 [11], which was one of the first applications of quantum mechanics to chemical kinetics.

One major difficulty in considering proton discharge is how to treat the very large total solvation energy of the proton (about −1,200 kJ mol^{-1}; [13]) which consists of the proton affinity of the water molecule to give the hydronium or hydroxonium ion, H_3O^+ (about 59% of the total), the so-called *inner-sphere* energy resulting from the orientation of the three-dimensional group of the closest water multipoles around this ion (about 26%) and the so-called *outer-sphere* energy due to the total energy of successive shells of oriented water multipoles at greater distances from the ion (15%). This has been modeled [14]. Gurney circumvented this problem by reducing all attractions to a single dimension in the form of a Morse function, which is replaced by a repulsive curve between the discharged proton and water of normal structure. According to the pre-Marcus view, a transition state analogous to that in a gas-phase reaction occurs in electron transfer, and solution species, with their aligned associated multipoles, can traverse the transition state barrier if they possess sufficient thermal energy. The exact model for the transfer of the electron in an electrochemical process involving discharge, charge, or change of valency was generally neglected. This view became changed among many electrochemists from 1956 onwards with the publication of the first seminal papers of Marcus [12, 15–17]. These dealt exclusively with heterogeneous (electrode) or homogeneous (inter-ion) electrochemical reactions involving valence change in redox species. The fundamental notion was that dimensional changes involving motions of the inner sphere solvent multipoles around the ion would occur, presumably by thermal activation, and sooner or later a configuration would occur with an intermediate configuration between the initial and final states of different valency. In the meantime, the outer sphere of solvent molecules, being decoupled from inner-sphere changes and only influenced by the central charge on the ion, would remain in its initial state. Assuming a charge transfer process at equilibrium, the reaction coordinate representing transfer of charge from the initial to the final state was represented by the intersection of two similar geometric curves with the *y*-axis representing free energy (see Fig. 1). The point of intersection above the initial-state energy is the free energy of activation of the process under equilibrium conditions. We must now determine the shape of the intersecting energy curves for reactants and products. Marcus considered that, when the inner sphere configuration reached the intersection point, an

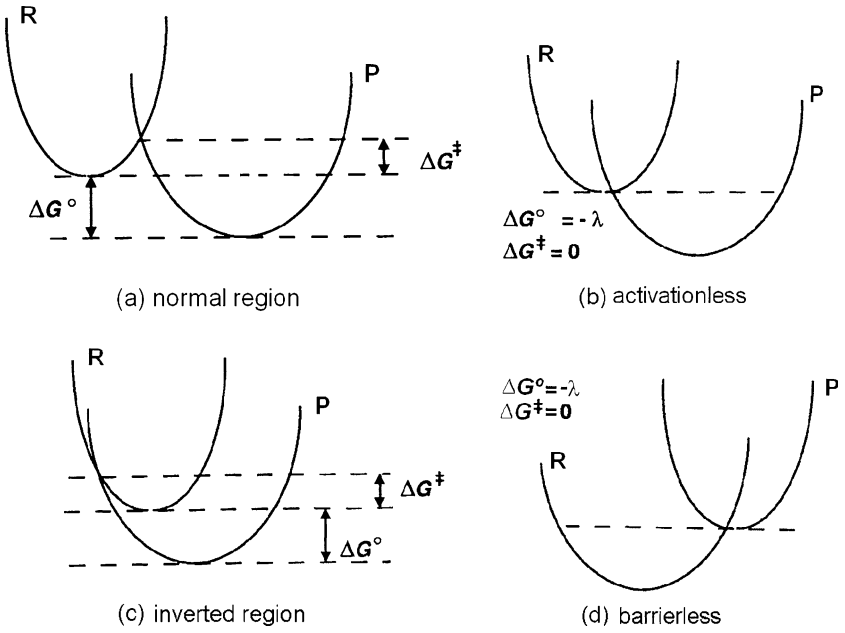

Fig. 1 **a**–**d** Potential energy surfaces for ET outer-sphere processes under different regimes. Adapted from Fig. 1.6 of [77]

electron would be transferred in a single rapid radiationless motion (ca. 10^{-15} s) either to or from the electrode or to or from the other ionic reactant (in the homogeneous electron transfer case). He considered the process to be generally adiabatic, i.e., any tunneling transmission coefficient is close to unity. During the very rapid transition of the electron, i.e., under "optical" conditions, it was supposed that any electronic polarization in solvent molecules in the outer sphere can keep up with the motion of the transferring electron. However, the inertial motion of the molecular multipoles cannot do this. The nuclear motions are thus frozen, and the process takes place in circumstances similar to the Franck–Condon (FC) approximation for spectral transitions first proposed separately by these authors in 1926 [18–21] or the equivalent Born–Oppenheimer approximation published in 1927 [22]. Marcus considered that the energies in the solvent on and after the transfer of the electron would be given by the Born charging equation [22] for the transfer of an electron from infinity to a point on the periphery of an ion, i.e., to a spherical condenser of the ionic radius, r. The Born equation has been a classic "equation of convenience" since its inception in spite of its physical deficiencies, which have often been pointed out [14]. These include the fact that the surface of an ion can hardly be treated as the external conduction surface of a spherical condenser, and the concept of bringing small elements of unit electronic charge from infinity to integrate a total change of charge makes no physical sense in quantum mechanical terms. However, the Born-derived relationship between change in energy and the change of charge between a medium of dielectric constant ε (the electrolyte) and of dielectric constant n^2 (the electrolyte at electron-optical frequency, where n is the refractive index at that frequency) has been widely employed and is:

$$\Delta G' = \left(z^2e^2/2r\right)\left(1/n^2 - 1/\varepsilon\right) = \lambda \tag{1}$$

where ΔG' is the change in free energy along a conceptual reaction coordinate in configuration space as the charge on the reactant goes to that on the product, where ze is the change in electronic charge (in which we may assume that $z=1$ since a simultaneous transfer of more electrons is of very low probability) and r is defined as the mean reactant–product radius modified if required by image charge effects in the electrode. In this case, $1/r$ is replaced by $1/r–1/R$, where R is twice the ion-electrode distance. In practice, the dimensional term was essentially an arbitrary radius adjusted to fit experimental results. The λ was called the reorganizational energy of the system. Marcus also considered a work-of-assembly term for the reactants. Finally, Marcus assumed that the free energy curves for reactants and products were parabolas (see Fig. 1) as a function of charge, which were shown to be geometrically similar. On this basis, the activation free energy of the process $\Delta G^{\ddagger}$ is equal to:

$$\Delta G^{\ddagger} = (\lambda + \Delta G_{\mathrm{d}})^2/4\lambda \tag{2}$$

where ΔG_{d} is the displacement of the parabola for the products from its equilibrium position, i.e., the displacement of the minimum free energy for the products from that of the reactants. ΔG_{d} can include both $F\eta$ for an electrochemical reaction and ΔG_{ads} for a Brønsted plot. The symmetry factor and Brønsted slope $\left(\mathrm{d}\Delta G^{\ddagger}/\mathrm{d}\Delta G_{\mathrm{d}}\right)$ are therefore $0.5 - (\Delta G_{\mathrm{d}}/2\lambda)$. Marcus assumed that the

frequency factor for the reaction was determined by the collision number. In latter papers, Marcus introduced an inner sphere term [23–25] and made an attempt to account for reactions with the breaking and making of bonds [26, 27], using the bond-energy–bond-order formalism [28]. In discussing the theory of Marcus, it is also necessary to discuss those of Hush [29–31] and Levich and Dogonadze [32–34]. The latter resulted in much the same formalism and energy expressions as that of Marcus, but in fact the basic physics is quite different. Dogonadze and Levich used a Hamiltonian description of the energy of the medium, derived from nonequilibrium thermodynamics rather than the classical electrodynamics used by Marcus. Unlike Marcus, they regarded the dielectric continuum as capable of activating the discharging ion via coupled harmonic electrostatic motions, with dipoles performing small oscillations around the discharging ion, each contributing one vibrational energy quantum of about 0.016 kT at 298 K for a frequency of 10^{11} s^{-1} or about 4×10^{-4} eV mol^{-1}. Thus, 1,300 dipoles would be required for the activation energy of 0.5 eV in a radius of 20 Å. This would correspond to a large polaron in the medium. They determined the electron transition probability using a time-dependent perturbation theory. They also considered other non-adiabatic phenomena involving tunneling transitions of the system. These theoretical approaches of Marcus and Levich–Dogonadze models may be called the *dielectric theories* of activation [35]. The alternative was a thermal theory of transition-state type. Because of the use of the harmonic approximation in the Dogonadze–Levich approach, with similar parabolic curves for reactants and products, the symmetry factor and Brønsted slope are the same as those in the Marcus theory. However, one major difference between the two theories is the fact that Dogonadze and Levich regard λ as an enthalpy of activation rather than as a free energy. The reasoning behind this is that it is experimentally temperature independent and is the difference between two free energies of charging with similar entropies. Finally, the Dogonadze–Levich theorists attempted to go beyond Marcus in attempting to explain the proton transfer process via simultaneous electron and proton tunneling from its solvation sheath to a metal surface, without accounting for water molecule reorganization [36]. This was reviewed in 1983 [37].

Theories with "flow of charge"

Hush assumed that, in electrode reactions, the eigenfunction of the electron transferred might flow as charge q from reactants to products over a relatively long time, with the ion–solvent interaction behavior governing the course of the (adiabatic) process. The simple ion–solvent interactions are a largely charge-independent energy of cavity formation in the solvent, the ion–dipole interaction depending linearly on charge and a Born charging energy depending on the square of charge. He did not consider induced dipole effects (also depending on the square of charge), which is reasonable because these occur at optical frequency. A further simplification was to ignore the effects of small changes in ligand–ion bond length, which is also implicit in the Marcus approach. The Born charging energy under static conditions for a change in charge of z to z–q is $(2qz-q^2)e^2(1-1/\varepsilon)/2r$ and that for the overall process $M^{z+}+e \leftrightarrows M^{(z-1)+}$ is $\left[z^2-(z-1)^2\right]e^2(1-1/\varepsilon)/2r$. The latter must be multiplied by q and subtracted from $(2qz-q^2)e^2(1-1/\varepsilon)/2r$ to give the change in energy ΔG^* along the reaction coordinate:

$$\Delta G^* = q(1-q)e^2(1-1/\varepsilon)/2r \tag{3}$$

where r is Bernal and Fowler's [38] Born radius of the ion (approximately the radius of the solvated ion). Differentiation shows that this has a maximum at $q^*=0.5$ so that the Gibbs energy of activation under equilibrium conditions is $e^2(1-1/\varepsilon)/8r = \lambda/4$, which for r=0.35 nm is about 49.6 kJ mol^{-1}, which is reasonable. Here the reorganizational energy λ is identical to that in the Marcus expression, Eq. 1, with $1/n^2$ replaced by 1. Adding $F\eta/RT$ to $\left[z^2-(z-1)^2\right]e^2(1-1/\varepsilon)/2r$ extends the expression to a net overpotential. Repeating the above procedure and differentiation now shows a maximum at $q^* = (\lambda + F\eta/RT)/2\lambda$. This is the same as the Marcus expression, leading to the same electrochemical symmetry factor and Brønsted slope. In a later paper, Hush [31] further developed his theory and compared it to that of Marcus. He took into account a change in ion–ligand distance in the inner sphere by adding a repulsive energy to the ion–dipole electrostatic term. The barrier height can be determined by binomial expansion as far as the quadratic terms (i.e., a harmonic approximation) to give the energy change along the reaction coordinate above the ground states of the reactants and products in equilibrium. Because quadratic terms are used, this also yields an expression identical in form to that of Marcus, so this does not change the symmetry factor and Brønsted slope. In the same paper, Hush modified his outer sphere energy equation by changing his original $(1-1/\varepsilon)$ term to the Marcus expression $(1/n^2-1/\varepsilon)$. His reasoning was that the electron transition time, though longer than that of the Marcus FC mechanism, would still be short compared to solvent molecule motion. The only effect of this is a change in the value of r to agree with the experiment.

The Hush theory has often been confused with that of Marcus and indeed has been called the Marcus–Hush theory. This might be due to the fact that the kinetic expressions of the

Hush theory and those of the Marcus (and of the Dogonadze–Levich theory under adiabatic conditions) are identical, but the physical models are quite different. Marcus and Dogonadze–Levich consider a reaction coordinate consisting of two identical intersecting upright parabolas, with FC transfer of the electron, whereas the Hush model consists of a barrier consisting of a single inverted parabola with charge transfer under non-FC conditions. The parabolas occur in both cases due to the assumption of a "harmonic approximation" for energy-configuration curves. In all cases, these theories result in curved Tafel and Brønsted plots. While the early work of Schmickler considered only the intersecting similar parabolas of the continuum theory, Koper and Schmickler stated in 1998 [39]: "For adiabatic reactions with strong coupling between the redox couple and the metal surface, electron transfer occurs gradually as the system moves along the reaction coordinate." This certainly suggests that, in electrocatalytic processes involving strong adsorption of intermediates, the concept of flow of charge must be invoked.

Inner sphere processes

The model for proton solvation has been discussed earlier. The most satisfactory model of an inner shell for higher valency ions (e.g., 2+, 3+) is as a "puckered" trikisoctahedron [13, 40, 41]. This has totally oriented water multipoles, which in turn have successive shells of solvent molecules with orientations determined by the local dielectric constant and dielectric displacement. For a 2+ ion, a model with a solvation energy of −1,852 kJ mol^{-1} was used, of which 56% was in the inner sphere, 15% in the "second sphere," and 29% in the dielectric continuum. For a +3 ion, the modeled value used was −4,496 kJ mol^{-1}, of which 50% was for the inner sphere, 15% for the second sphere, and 35% for the dielectric continuum [42]. We note that the dielectric constants between r and ∞ in Eq. 1 are assumed to be constant as a function of r. This is true for n^2, but speculative for ε close to the ion. In general, most authors have used the bulk value of ($\varepsilon=\varepsilon_0$) and have ignored possible dielectric saturation near the ion. In any case, for water, the value of $1/\varepsilon_0$ is negligible. However, the Booth [43] model of the vector sum of the dielectric counter-displacements CA_A that constitute a dielectric constant can be modified to give a very useful correlation function between the local dielectric constant ε_A and the local dielectric displacement, A_A. Thus, $\varepsilon_A=A_A/A_A-CA_A$. The correlation function is:

$$\varepsilon_A = \left(\varepsilon_0^2 - 2bA_A{}^2\right) \tag{4}$$

where b is derived from the Langevin function for the angle of inclination to the electric field of a water molecule (approximated to be a dipole) from its mean thermal disorder angle (z). For water at ordinary temperatures, b is about 3.15×10^{-9} in units of esu^{-2} cm^4 with A_A in esu cm^{-2} (these now-obsolescent units are used because of their convenience and simplicity in calculating intermolecular and interionic interactions).

Finally, the validity of Eq. 1 must be decided. Its physics as originally discussed by Born is certainly flawed; however, a more complete analysis [13] shows that the outer-sphere or *electrostatic continuum* energy can be correctly determined by a summation (not an integration) of the energy contributions of successive shells of solvent molecules, taking into account, when required, the Langevin modification of the bulk dielectric constant. This treatment does not require the very dubious assumptions of the Born charging energy. However, it leads to the same result as the latter if the summation is replaced by an integration from infinity up to a certain effective value of r. Thus, this does not change the implications of the energy given by Eq. 1.

Tafel plots

Tafel plots are an experimental observation and are therefore worthy of acceptance under the Baconian view of physical observation, as distinct from one derived from Ptolemaic reasoning. Khan and Bockris [44] have reviewed the evidence for the experimental existence of "linear" Tafel plots for various electrochemical reactions as distinct from the "curved plots" characteristic of outer sphere or "electrostatic theory" processes.

If a Tafel plot is a real physical entity, it implies one particular characteristic of an electrochemical kinetic process. Any such reaction must have a rate-determining step, which as in conventional chemical kinetics may be characterized by the occurrence of an intermediate reactant species on an energy barrier which must be traversed to go to the next stage of the process. This rate-determining step (rds) must have a particular partial electronic charge, which must remain constant no matter what the reaction overpotential happens to be. We may illustrate this point by considering a simple redox reaction, e.g., the overall process $M^{z+} + e^- \leftrightarrows M^{(z-1)+}$ considered earlier. Without modeling the reaction coordinate energy change, we may state ab initio that, if there is a transition state in this reaction, then the reactant (M^{z+}) must be energized, presumably by a Boltzmann thermal mechanism, to an energy to surmount the barrier. At this point, the electron is accepted in *radiationless* transfer process to its free energy value in the metal Fermi energy. The excited product ion $M^{(z-1)+}$ then gives up its thermal energy by collisional energy loss to the molecular bath. The electrochemical

potential of the electron produced in the electrode of course remains at the energy of the transition state. So far, we have not determined if the reaction proceeds by an FC process, as in Marcus and Levich–Dogonadze, or by *flow of charge*, from reactant to product, as in Hush [29]. If one accepts the former view, then for a reactant activation to an energy under the barrier, no electron transfer at all can occur, in which case the process will be unsuccessful. If one accepts Hush's *flow of charge* view, a similar reactant activation will result in a partial, but unsuccessful, charge transfer, which will be reversed, with the partially activated reactant returning to the thermal bath after deactivation by collisions. Partial change transfer is defined as a state in which the multipoles associated with the change in charge are in their equilibrium positions, both in the "inner" and "outer" spheres. It is evident that the change in induced dipole effects throughout the system adjacent to the ion will also be in equilibrium while the transfer process occurs.

We must now consider the effect of changing the Fermi energy of the electrode by applying a potential difference. If such a bias potential is applied, it will supply electrons with that potential difference to the transition state at the top of the barrier. The potential change does not affect the free energies of the reactant or product in the solution or that of the transition state at the top of the barrier. It simply provides a sliding scale compared with that of the barrier so that the barrier is shifted with regard to the Fermi energy. This suggests that the shape and charge on the barrier is in effect unchanged by the application of overpotential. This may indeed be the origin of an effectively constant Tafel slope. The Marcus–Dogonadze–Levich FC concepts and the Hush "flow-of-charge" concept may well yield a symmetry factor (and by inference, a Brønsted factor) of 0.5 by the use of a harmonic approximation. However, a more realistic evaluation for the "flow-of-charge" case, taking into account the real motions of the "inner sphere" during charge transfer and using the fact that the inertial motions of the "outer sphere" (the Langevin angles for individual radial solvent molecules shells) will keep up with these, will maintain that only inner sphere reorganization contributes to the activation energy [13]. These real displacements result in a possible variation of the symmetry factor from the usual approximation of 0.5 at equilibrium.

One interesting problem is what happens to reactions at very high overpotentials. For the electrostatic continuum assumptions for a solvent coordinate consist of intersecting similar parabolas (Equation 2), which may be written $\Delta G^{\ddagger} = (1-n)^2/4\lambda$ with a corresponding symmetry factor $\beta = 0.5 - n/2$, where $\Delta G_d = n\lambda$. We assume a cathodic process, i.e., the parabola for the reactants is displaced with change in electrode potential. Since metal electron levels are inverted compared with positive ion levels in solution, a positive energy change results in a reduction of activation energy (see Fig. 2).

For $n=-1.0$, $\Delta G^{\ddagger} = +\lambda$, and the base of the parabola for the reactants intersects with the side of that of the products at a height λ above the reactants in the initial ground state (see Fig. 1). The activation energy barrier, as such, has now disappeared, and $\beta=1.0$. Such processes have been called *barrierless* (see Fig. 1). Barrierless processes will be strongly endothermic. As n further increases, a barrier now reappears on the opposite side of the parabola for the products (see Fig. 1), so both $\Delta G^{\ddagger}$ and β also continue to increase, with the other kinetic factors remaining the same.

Conversely, for $n=+1.0$, $\Delta G^{\ddagger} = 0$, and the base of the parabola for the products is intersected by the "leg" of that of the products. β is now zero. Such processes have been called *activationless* (see Fig. 1) and would have the nature of a very rapid chemical-limiting current, probably greatly exceeding the diffusion-limiting current for the process in question. Such reactions will be strongly exothermic. For $n>-1.0$, an activation energy barrier starts to reappear on the other side of the reactant barrier from that facing the products. In this case, β is now relatively small and negative (e.g., for $n=-1.2$, $\beta=-0.1$). This has been called the *inverted region* and is discussed further down (see Fig. 1).

The concept of barrierless and activationless FC processes based on Dogonadze–Levich continuum theory was first introduced by Krishtalik in 1959 [45]. It is most accessible in a 1983 review [44]. Krishtalik studied the possibility of barrierless transfer for hydrogen evolution on metals such as mercury, on which the free energy of hydrogen atom adsorption is highly positive even at the normal overall hydrogen equilibrium potential. It is assumed above that, for overpotentials beyond the barrierless region, the activation energy will continue to increase and the reaction rate to

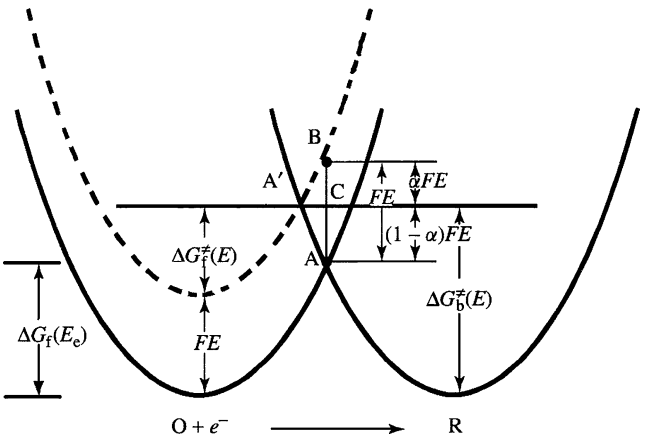

Fig. 2 Effect of electrode potential on the free energy versus coordinate curves for an electron reactant at two electrode potentials: $E = Ee$ and $E < Ee$ (*broken line* parabola). Reproduced from Fig. 2 of [65] with permission from Wiley

decrease. However, Krishtalik shows that in fact electrons will no longer be transferred mostly from the equilibrium Fermi energy of a metal electrode, but from excited levels on higher electron energy than the Fermi energy. Similarly, for overpotentials beyond the activationless region, the electron will be transferred from fully populated levels under the Fermi energy. The mean population of the level supplying an electron is given by $1-\beta$ so that, at the reaction level of $\beta=1/2$, it is the Fermi energy, at $\beta\rightarrow 0$ it is an underpopulated excited level and at $\beta\rightarrow 0$ it is a (negatively) lower, filled level. Thus, Krishtalik maintained that the regions appearing on the far side of the parabolas will make essentially no contributions to extreme reaction rates.

The Marcus approach did not consider the electron energy at overlap, so the inverted region remained a possibility. According to the Marcus model, on a plot of log k versus $-\Delta G°$ of the reaction, for small driving forces the correlation is linear, but for larger driving forces a maximum activity should be observed at $\Delta G°=-\lambda$, where λ is the outer-sphere reorganizational energy (see Fig. 1). For driving forces beyond this value log k decreases, giving rise to what has been called the "inverted region" (see Fig. 3)

Experimental evidence for this behavior was elusive for many years since the first papers published by Marcus in 1956 as very large values of k could not be measured due to mass transport limitations since the electron transfer rates were much faster than the rates of diffusion of reactants. In 1985, Miller, Closs and Calcaterra [46] published some experimental evidence of the existence of an "inverted region" for a reaction taking place in the homogeneous phase (this was not an electrochemical reaction). In this work, any mass transport limitations were solved by placing the electron donor and electron acceptor in the same molecule separated by a bridge (see Fig. 3). Even though in the literature it is claimed that [46] was the first paper to demonstrate experimentally the existence of the inverted region, in 1982 a similar evidence was shown by Kadhum and Salmon but has been rarely cited [47]. In outer-sphere electrodic reactions occurring on metallic electrodes, an inverted region is not observed since the electrode has closely spaced electronic states and levels above and below the Fermi energy are also available like many closely packed parabolas on the left of Fig. 2. However, it is possible to observe an inverted region on a metal electrode if the redox species is well separated from the surface of the electrode by self-assembled monolayers (SAMS) of alkane thiols acting as spacers between the electrode and the redox center [48]. This drastically reduces the electronic coupling between the electrode and the reacting species. For example, the right side of Fig. 3 shows the results for the oxidation of cytochrome c as reported by Bowden et al. [49]. Curved Tafel lines on gold electrodes coated with SAMS as those illustrated in the right side of Fig. 3 were first observed by Chidsey [48] and this triggered many studies using SAMS, in some cases to mimic ET processes in biological systems [50–52]. All of these findings have proved that, as discussed by McLendon and Hake, "electron-transfer reactions can occur at reasonable rates even when the reactants are separated far beyond collisional distances. Under optimal circumstances, rates of 10^6 s^{-1} can be obtained even when the electron donor and electron acceptor are separated by ca 10 Å of intervening solvent" [50]. This is a situation similar to that depicted in Fig. 3a for donor and acceptor separated by a bridge. Kakitani and Matanaga [53] have proposed a modification of Marcus theory. They have suggested that, due to dielectric saturation in the first solvent

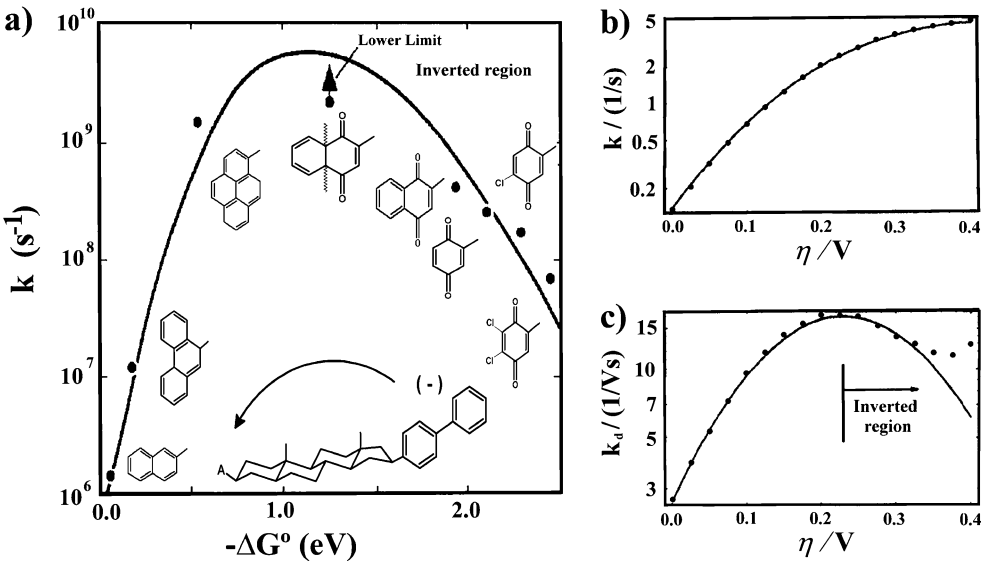

Fig. 3 **a**–**c** *Left*, plot of log k versus driving force for the intramolecular electron transfer in molecules depicted in the figure. *Right*, plot of log k versus overpotential for the oxidation of cytochrome c immobilized on SAMS of thiols on gold. Adapted from [47] and [50]

shell around ionic compounds, the curvature of the energy surfaces should be larger for ion pairs than for neutral or slightly charged species. Fletcher has also proposed a different model to account for deviations in the inverted region [54–56]. Fletcher's model was extended [55] not only to highly exergonic reactions (the inverted region where $\Delta G°<-\lambda$) but also to highly endergonic reactions (the superverted region, where $\Delta G°>\lambda$). The mathematical derivation, in the form of Gibb free energy profiles, was plotted versus a charge fluctuation coordinate (see Fig. 4). This new model uses the concept of donor and acceptor "supermolecules" consisting of donor and acceptor species and their associated ionic atmospheres. As discussed by Fletcher: "The key findings are as follows. (1) In the inverted region, donor supermolecules are positively charged both before and after the electron transfer event. (2) In the normal region, donor supermolecules change polarity from negative to positive during the electron transfer event. (3) In the superverted region, the donor supermolecule is negatively charged both before and after the electron transfer event (see Fig. 4). This overall pattern of events makes it possible for polar solvents to catalyze electron transfer in the inverted and superverted regions" [55]. This new effect is predicted only by the Fletcher's model and not by the earlier Marcus theory and provides a clear means of distinguishing between these two theories.

The Tafel equation

If we now concentrate our attention on reactions taking place at an electrode interface, the most essential linear Gibbs free energy correlation in electrochemistry is the empirical Tafel equation discussed above and consequently the Butler–Volmer equation describing overall kinetics in the anodic and cathodic directions.

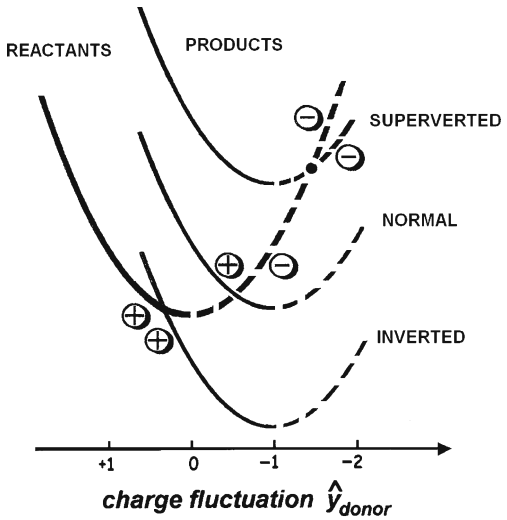

Fig. 4 Superverted ($\Delta G° < -\lambda$), normal ($-\lambda < \Delta G° < \lambda$), and inverted ($\Delta G° < -\lambda$) regions for ET in nonpolar solvents according to Fletcher [55]. Reproduced with permission from Springer

The classical seminal paper of Tafel [57] in 1905 essentially gave birth in electrochemistry to an era of quantitative interpretation of electrode kinetics where for the first time a correlation was established between current density and overpotential, i.e., a correlation between the rate of a reaction and the driving force. Tafel found an empirical linear correlation between the logarithm of current density and the overpotential for the hydrogen evolution reaction on several metals including Cd, Pb, and Hg. While the reactivity towards hydrogen evolution depended on the nature of the metal, the concept of electrocatalysis was not known at that time.

The Tafel equation, using modern notation, is

$$\eta = a + b \log i \tag{5}$$

In the original paper, the overpotential η was "ε" and the current density i was "j". A recent, very interesting detailed discussion of the Tafel equation has been published by Tsirlina et al. [58]. A very good discussion of the Brønsted–Tafel relation has been presented by Hupp and Ram [59].

The equation that describes the dependence of log i on the overpotential is the Butler–Volmer rate equation. This describes a linear correlation between the energy of activation and the electrochemical free energy of the reaction. This is a phenomenological equation and has been derived from "first principles" by Schmickler and Koper [39], the same being the case with the Tafel equation as described by Fletcher [60]. The current is the total current, which is measured experimentally and considers both reduction and oxidation processes. The left-side term inside the brackets considers the oxidation (the reaction is triggered by holes on the electrode) and the term on the right considers the reduction (the reaction is triggered by electrons. Note that we use α for transfer coefficients and β for symmetry factors and Brønsted coefficients):

$$\begin{aligned} i &= i_{\mathrm{red}} - i_{\mathrm{ox}} \\ &= nFk^0\left[C^{\mathrm{s}}_{\mathrm{red}} \exp \alpha \frac{nF}{RT}\eta - C^{\mathrm{s}}_{\mathrm{ox}} \exp(1-\alpha)\frac{nF}{RT}\eta\right] \end{aligned} \tag{6}$$

$$i = i_0\left[\exp -\alpha \frac{nF}{RT}\eta - \exp(1-\alpha)\frac{nF}{RT}\eta\right] \tag{7}$$

C^{s} is the concentration of oxidized or reduced species in the bulk electrolyte.

This equation will be true provided that the Butler–Volmer reaction is a valid kinetic description of the overall process, i.e., the reaction is quasi-reversible with the same

rate-determining step in both the anodic and cathodic directions. We should note these are the "traditional" pre-1956 forms of the Butler–Volmer equation, which do not take into account the reaction mechanism, and still sometimes appear in textbooks and other publications. The equations may be generalized by replacing $(1-\alpha)n$ and αn by α_a, α_c, where these are the anodic and cathodic transfer coefficients. At low coverage, a general expression derived in 1956 from the pseudo-equilibrium assumption [61] is that $\alpha_a = n_a + \beta$, and $\alpha_c = n_c + (1-\beta)$, where β is the symmetry factor in the rds, which is approximately 0.5 (see earlier discussion of charge transfer), and n_a and n_c are the number of electrons transferred in pseudoequilibria before the rate-determining step in the anodic and cathodic directions, respectively. These relationships assume that only one electron is transferred in each unit of the rds (or, in the case of a chemical rds, zero electrons) since the transfer of two or more electrons is quantum-mechanically extremely improbable. The reorganizational energy λ for the rate-determining steps involving more than one electron should also be very high and unlikely. However, some authors sometimes propose reaction mechanisms with the rds involving more than one electron without realizing these fundamental limitations. Thus, in general, in reactions involving Langmuir adsorption of reactants or intermediates at low coverage, $\alpha_a + \alpha_c = n$, the total number of electrons involved per unit of the rate-determining step. It may be shown that this is also true in the more complex cases of medium and high coverage.

Both terms inside the brackets in Eqs. 6 and 7 have similar weight only at small overpotentials (linear polarization region), but this will also depend on the value of the exchange current density i_o. The features of the polarization curve described by the Butler–Volmer equation will depend on the value of i_o. So, when the system is far from equilibrium, only one term is important. For example, for positive overpotentials, i.e. anodic polarization, the reaction is triggered by holes on the electrode and the Butler–Volmer equation becomes:

$$i = i_o \exp(\alpha_a F \eta / RT) \tag{8}$$

where α_a is the anodic transfer coefficient. Rearranging it gives:

$$\eta = \log i(2.303RT/\alpha_a F) - \log i_o(2.303RT/\alpha_a F) \tag{9}$$

which is similar to the Tafel equation, where $a = \log i_o (2.303RT/\alpha_a F)$ and $b = (2.303RT/\alpha_a F)$, with b being the well known "Tafel slope" that provides information about the mechanism of the reaction, specifically, about the rate determining step. For $n=1$ (number of electrons transferred) and for a transfer coefficient $\alpha = 0.5$, the absolute value of the slope is close to 0.120 V/decade at 298 K, which is a typical value for reactions involving the transfer of one electron and the electron transfer process is rate determining (we use the absolute value of the slope because for cathodic processes the slope is negative). For multiple electron transfer reactions $|b|$ is also ca. 0.120 V/decade if the transfer of the first electron is rate determining. Fletcher has recently published a paper that summarizes a series of possible electron transfer mechanisms and the corresponding Tafel slopes that should be observed [60]. Both the Tafel and Butler–Volmer correlations are applicable if the electron transfer process studied is not affected by other electrodic parallel processes and that double-layer effects are negligible. As stated by Tsirlina et al. [58]: "It is assumed that there are no parallel reaction pathways, and the rate determining step is presented by the charge transfer process with the participation of reactant having a fixed bulk concentration, not an intermediate species". The Tafel slope (when using $\log_{10}$ rather than ln) essentially tells us the amount of driving force (in volts) that is required to increase the rate of the reaction by a factor of 10. Hence, the lower the Tafel slope the better in terms of the energy required to increase the rate of the reaction by changing the electrode potential. For a given reaction, the Tafel slope can have different values depending on the nature of the electrode employed and the mechanism of the reaction on that particular electrode.

The hydrogen discharge and evolution reaction

This is the archetypical reaction in electrocatalysis and more details can be found in several textbooks and reviews [2, 62–67]. It is interesting to quote: "An overly obsession with hydrogen evolution has delayed the development of electrochemistry by at least a decade" according to Bockris as cited by Schmickler [64]. "Unfortunately, the hydrogen electrode must be considered to be an extremely complicated example. This may be well the reason for the relatively slow development of electrode kinetics", according to Vetter as cited by Schmickler et al. [64].

The following mechanisms have been proposed for it, with two options for the second step: $H^+ + e^- \rightarrow H_{ads}$ step 1 (discharge or Volmer reaction), $H_{ads} + H^+ + e^- \rightarrow H_2$ step 2a (electrochemical desorption or Heyrovsky reaction), and $H_{ads} + H_{ads} \rightarrow H_2$ step 2b (combination or Tafel reaction). If step 1 is rate determining, the Tafel slope should be 0.120 V/decade at 298 K. If step 2a is rate determining, the slope should be 0.040 V/decade, and if step 2b is rate determining, the slope should be 0.030 V/decade (a chemical step, following two rapid electron transfers). All of these assume Langmuir adsorption at low coverage. This is graphically illustrated in Fig. 5. We have intentionally drawn this plot with the electrode potential on the x-axis so as to

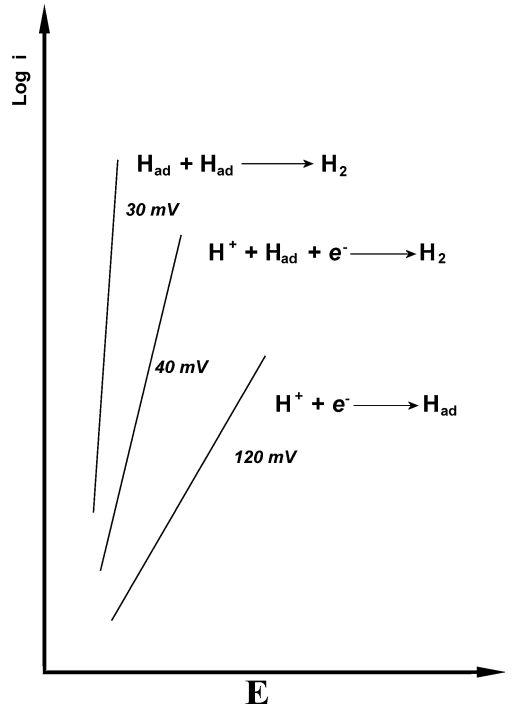

Fig. 5 Hypothetical Tafel plots for hydrogen discharge for different ET mechanisms. Note that, since $b=dE/dlogi$, the steeper *straight line* is the one with the smallest Tafel slope

emphasize that this represents the electrode driving force; so, for the lower Tafel slope, the rate of the reaction is more sensitive to the increase in driving force. In electrocatalysis, a lower Tafel slope is better since the voltage of a cell (producing electrical energy) will decrease less with polarization compared to the case where the Tafel slope is larger.

At reasonably high overpotentials, the hydrogen discharge and evolution reaction (HER) mechanism can be characterized by the two sequential Volmer and Heyrovsky reactions. The reason for this is the fact that the Tafel reaction is non-electrochemical, even though it is preceded by the electrochemical Volmer proton discharge reaction, which governs the coverage of the Tafel reactant, adsorbed hydrogen. Hence, its rate at constant coverage is independent of overpotential, and the Heyrovsky electrochemical proton plus adsorbed hydrogen stripping reaction soon exceeds the chemical rate of the Tafel reaction. An evaluation of the combined sequential Volmer and Heyrovsky reactions is instructive. The procedure given below is based on the electrochemical steady-state procedure of Bockris and Mauser [68] and is adapted from [69].

Santos and Schmickler [70] have stated that the outer-sphere continuum theories were "sometimes applied to reactions which were definitely not outer sphere, such as metal deposition or hydrogen evolution." They have attempted to go beyond this, but they still assume an FC dielectric continuum theory for the reorganizational energy. However, they have used computational approaches (density functional theory, DFT, calculations) to the free energy of adsorption on metal electrodes, with some success for the proton discharge process.

We first accept the existence of a Brønsted effect for the Gibbs free energy barriers for each of the two charge transfer processes, whose equilibrium rate constants are k_1 and k_2. In the Volmer reaction, the solvated proton with charge 1+ becomes an unsolvated and adsorbed hydrogen atom (H_{ads}) with zero charge. The free energy of adsorption of the discharging proton varies from zero to ΔG_{ads} along the reaction coordinate. If the charge on the Gibbs free energy barrier at its apex (i.e., at the transition state) is β_1+, then the Gibbs free energy of adsorption at the transition state is $-(1-\beta)\Delta G_{ads}$. This results in an equilibrium rate constant of $k_1\exp-(1-\beta)\Delta G_{ads}/RT$ for the Volmer reaction, which varies with cathodic overpotential η (considered negative) by the Tafel multiplier $\exp-\beta F\eta/RT$. The forward rate of the reaction is therefore:

$$[H^+](1-\theta)k_1\exp-(1-\beta)\Delta G_{ads}/RT\exp-\beta F\eta/RT \quad (10)$$

where $[H^+]$ is the proton activity in the solution and θ is the coverage of active sites by (H_{ads}). All such sites are considered equal from the viewpoint of adsorption energy, which is an oversimplification to be examined later. The backward Volmer process with $\Delta G_{ads}=0$ has an equilibrium rate of θk_1 and the adsorbate sees a barrier height increased by $\Delta G_{ads}-(1-\beta)\Delta G_{ads}$, i.e., $+\beta\Delta G_{ads}$. The rate of the back reaction is therefore:

$$\theta k_1\exp+\beta\Delta G_{ads}/RT\exp+(1-\beta)F\eta/RT \quad (11)$$

Corresponding arguments show that the forward and backward rates of the Heyrovsky reactions are:

$$[H^+]\theta k_2\exp-(1-\beta_2)\Delta G_{ads}/RT\exp-\beta_2 F\eta/RT \quad (12)$$

$$[pH_2](1-\theta)k_2\exp+\beta_2\Delta G_{ads}/RT\exp+(1-\beta_2)F\eta/RT \quad (13)$$

where $[pH_2]$ is the hydrogen partial pressure and β_2 is the corresponding Brønsted coefficient and symmetry factor for the Heyrovsky reaction. The overall rate is equal to that of each of the forward and backward pairs of reactions, and the condition for a steady-surface adsorption state is that $d\theta/dt=0$, i.e., the rates of reactions (10) − (11) − (12)+(13)=0. This allows the calculation of general expressions for θ and the overall rate k as a function of the overpotential and ΔG_{ads}. While not necessary, the simplification $\beta_1=\beta_2=0.5$ is convenient to see the general trends. The results are:

$$\theta=\left\{[H^+]k_1A^2+[pH_2]k_2\right\}B^2/Q \quad (14)$$

$$k=k_1k_2B\left([H^+]A^3-([pH_2]/A)\right)/Q \quad (15)$$

where k is the net reaction rate and $Q = k_1([H^+]A^{\,2}B^{\,2} + 1) + k_2([H^+]A^2 + [pH_2]B^2)$, $A = \exp -F\eta/2RT$, and $B = \exp -\Delta G_{ads}/2RT$. This analysis shows the difference between the "dynamic isotherm"

$$\theta/(1-\theta) = \left\{[H^+]k_1A^2 + [pH_2]k_2\right\}B^2/\left(k_1 + [H^+]k_2A^2\right) \quad (16)$$

compared with the "static" values:

$$\theta/(1-\theta) = [H^+]A^2B^2 = [pH_2]B^2/[H^+]A^2 \quad (17)$$

Thus, if the terms containing k_2 are small compared with those containing k_1, the second step is rate-determining and $\theta/(1-\theta) = [H^+]A^2B^2$. If the contrary is true, $\theta/(1-\theta) = [pH_2]B^2/[H^+]A^2$ and the first step is rate-determining.

A useful simplification of Eqs. 10–13 can be made by ignoring the back reactions, which will be reasonable at overpotentials of about −0.1 V, and regarding the $[H^+]$ and $[pH_2]$ reactant activities as being equal to unity. Q is then simply $A^2(k_1B^2 + k_2)$, θ is $k_1B^2/(k_1B^2 + k_2)$, and:

$$k = k_1k_2AB/\left(k_1B^2 + k_2\right) \quad (18)$$

Thus, we find that θ is independent of overpotential, and for large B^2, i.e., large $\exp -\Delta G_{ads}/RT$ or large negative ΔG_{ads}, it is close to unity. The overall rate k is then k_2A/B, i.e., the Tafel exponential factor is $\exp -F\eta/2RT$ and the Brønsted exponential factor is $\exp +\Delta G_{ads}/2RT$. The occurrence of k_2 in the rate equation means that the Heyrovsky reaction is then rate determining. For small B^2, i.e., for large positive ΔG_{ads}, the rate is k_1AB and the Volmer reaction is therefore rate determining. The Tafel slope is still $\exp -F\eta/2RT$ but the Brønsted slope is now $\exp -\Delta G_{ads}/2RT$. Thus, we have a "volcano" relationship between ln k and ΔG_{ads}, with a rising branch on the positive ΔG_{ads} side and a falling branch on the negative side. This may be interpreted as an example of the so-called *Sabatier principle* [71] of catalysis (after Paul Sabatier, Nobel laureate), in which catalytic rates over a series of materials increase with decreasing (negative) free energy of adsorption and coverage, then these fall with increasing negative free energy of adsorption, giving an optimum rate at some intermediate value.

Catalytic effects in electrochemistry

Many electrochemical reactions involving reactants in the solution phase proceed at reasonable rates at potentials that are removed from the equilibrium potential, i.e., they require a significant overpotential to occur at measurable rates due to the slowness of the electron transfer and chemical steps associated to the process. This is the case of many electrochemical reactions of interest that usually require the transfer of more than one electron. The slow step can be accelerated by the action of electrocatalysts in two ways:

1. The catalyst can be present in the solution phase, in which case the electrode serves only as a sink or source of electrons.
2. By a heterogeneous process where the catalysts can be the electrode surface itself (most d-type noble metals such as Pt, Pd, etc.) or a catalyst confined to the electrode surface (i.e., for so-called modified electrodes).

1. The catalyst is present in the solution phase.

For case 1, we first acknowledge that the homogeneous catalytic process may proceed in two different ways: the outer-sphere and inner-sphere mechanisms. For the outer-sphere mechanism, the process has been termed "redox catalysis" and the active form of the catalyst is continuously re-generated at the electrode surface and exchanges electrons with the reactant via an outer-sphere process. The catalyst and the reactant only collide in the homogeneous phase but do not form a bond. The catalyst which can be oxidized or reduced after exchanging electrons with the reactant recuperates its initial oxidation state at the electrode surface. The catalysis in this case is a physical phenomenon since the lowering of the overpotential of the reaction results from the three-dimensional dispersion of the mediator. The driving force of the reaction is provided by the redox potential of the catalyst and not by the potential of the electrode, which only regenerates the active form of the catalyst at the interface (no reaction takes place directly between the electrode and the reactants and, strictly speaking, the electrode provides the driving force to regenerate the active catalyst). For the case of an "inner-sphere" process, should this exist, it is "chemical catalysis" and involves the temporary formation of an adduct between the mediator and the reactant. The bond formed between the catalysts and the reactant is broken after the exchange of electrons to give intermediates and products, regenerating the initial from of the catalyst.

For example, for a reduction reaction mediated by catalysts present in the solution phase, on thermodynamic grounds, it is expected that the more negative the formal potential of the mediator (more powerful reductant) the higher its reactivity for the oxidation of the target, according to the reaction scheme below, where step 21 is rate determining:

$$[cat] + e^- \quad \rightarrow \quad [cat]^- \quad (19)$$

$$[cat]^- + \text{target} \rightarrow [cat] + \text{reduced intermediate}. \quad (20)$$

$$\text{reduced intermediate} \rightarrow \text{products} \quad (21)$$

This is true for homogeneous outer-sphere redox catalytic processes, where both the mediator and the reacting molecule are present in the homogeneous phase, and no bond between the mediator and the target molecules is formed. The reactivity, plotted as log k, where k is the rate constant of the rds, versus the formal potential of the mediator gives a straight line of positive slope. This has been demonstrated in a series of papers by Savéant and coworkers [72–75] and reviewed in books [76, 77]. The same authors have shown that, if a bond is formed between the catalyst and the target molecule, such as reaction 4 (inner-sphere process), the observed reactivity of the catalysts is much higher than that predicted by its redox potential.

$$[\mathrm{MPc}]^{+} + \mathrm{target} \rightarrow [\mathrm{MPc}\ldots\mathrm{target}]^{+} \quad (22)$$

The reaction studied involved the rupture of a bond so Marcus model cannot be applied but rather a modified version proposed by Savéant that describes a Morse curve rather than a parabola for the reaction products [72–76]. A model for dissociative electron transfer was first proposed independently by Savéant [78, 79] and by German and Kuznetsov [80]. These models are interesting extensions of models for outer-sphere reactions, where a bond-breaking coordinate is introduce with simple model potentials. Dissociative electron transfer processes involving organic molecules has been also studied by Maran and Workentin [81–83]. This has been developed further for the bond-breaking electron transfer of diatomic reactants at metal electrodes by Santos, Koper, and Schmickler [84] using a model Hamiltonian for concerted bond breaking and ET reactions, combining elements of Marcus theory and the Anderson–Newns model, and tight binding. In an earlier work, Koper and Voth [85, 86] reformulated Savéants' theory using a Hamiltonian model. This allowed the exploration of quantum effects such as tunneling transitions and Frank–Condon effects.

Figure 6 illustrates the dependence of log k versus the formal potential of the catalyst for the reduction of *trans*-1,2 dibromocyclohexane by aromatic radicals and by reduced metalloporphyrins. The catalysts that fall on the straight line, according to the previous discussion, promote the reaction via an outer-sphere mechanism whereas those that show higher activities than those predicted by their formal potential escape from the linear correlation. In the latter, the catalytic effect rises from the formation of an adduct between the reacting molecule and the catalyst, which lowers the activation energy of the process. The slope of the line is −0.130 V/decade, which is similar to a Tafel slope.

2. The catalyst is confined on the electrode surface.

For this case, the catalyst can be the electrode surface itself of catalysts confined on its surface. In this case, the phenomenon is well-known as "electrocatalysis". The first

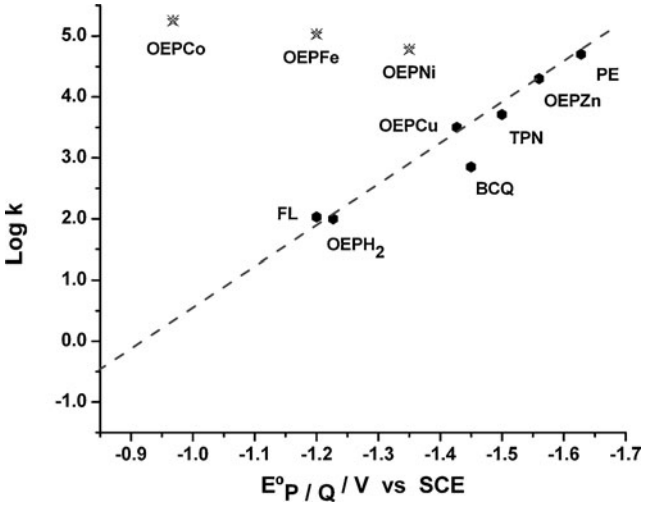

Fig. 6 Plot of log versus the redox potential of several catalysts present in the homogeneous phase for the reduction of *trans*-1,2 dibromocyclohexane. Driving force increases to the right. Adapted from Fig. 7.1 of [77]

references to "electrocatalytic reactions" were made by Kobosev and Monblanova 1934 and 1936 [87, 88]. Electrocatalysis (reviewed in [66]) involves "inner sphere" electron transfer processes that occur at electrode surfaces where the reacting species or intermediates adsorb on the electrode surface. The kinetics of these reactions, analogously to heterogeneous catalytic, are very sensitive to the nature and structure of the electrode surface. An example of this are the HOR/HER reactions already discussed in the previous section. Outer-sphere and inner-sphere ET reactions can be affected by the nature of the electrode surface, for example, for metals due to the effect of the density of states at the Fermi energy. The same is true for reactions taking place at semiconductor interfaces, where the ET rates are reduced because of the forbidden gap that affects the effective surface electron concentrations. These effects however are not electrocatalytic and are only due to electronic factors [66].

Most electrode processes that are of industrial interest involve electrocatalytic phenomena, such as the production of chlorine in the chloro-alkali cell, the electrochemical splitting of water to give hydrogen and oxygen gas, oxygen reduction and hydrogen oxidation in H_2/O_2 fuel cells, and the electrooxidation of fuels in general just to mention a few. Reactions of vital importance are also the oxidation of methanol and of CO and the electroreduction of CO_2. The list is long and it is well beyond the scope of this manuscript. Instead we might give an overview of the evolution over the years of the level of understanding of catalytic processes in terms of reaction mechanisms, electrochemical Tafel correlations, volcano correlations, and the introduction of spectroscopy as a powerful tool to understand the chemistry of electrocatalytic processes.

Volcano plots

Volcano correlations are observed in heterogeneous catalysis, where the catalytic activity is compared to some parameter that indicates the degree of interaction of reactants or intermediates with the surface of the catalyst. This comes from the old concept introduced by Sabatier in 1911 [71] as mentioned before that, to obtain the highest catalytic activity, the interaction of the molecules on the surface needs to be not too weak and not too strong. Volcano correlations are very important in describing the phenomenology of heterogeneous catalysis. They describe trends in reactivity that are very helpful in designing more active catalysts. In electrocatalysis, most studies have been focused on the catalytic activity of pure metals, alloys, or oxides. For example, the well-studied hydrogen evolution reaction [89] was first studied by Tafel in 1905, when he established his famous equation [57]. Essentially, the correlations between the exchange current density and the free energy of adsorption ΔG_{ads} of hydrogen on the surface of the electrode (when comparing different electrode materials) have a volcano shape (see Fig. 7). This has been demonstrated experimentally by many authors and was reviewed by Trasatti in 1972 and 1994 [90, 91].

The shape of the volcano curve was explained independently by Gerischer and Parsons in 1958 [92, 93] who deduced that i_o is related to the standard Gibbs free-energy for hydrogen adsorption $\Delta G°_{ads}$. Figure 7 shows a rather recently published volcano correlation by Nørskov et al. [94] where experimentally measured i_o values for hydrogen evolution are compared versus $\Delta G°_{ads}$ calculated theoretically using the density functional theory (DFT). The curve

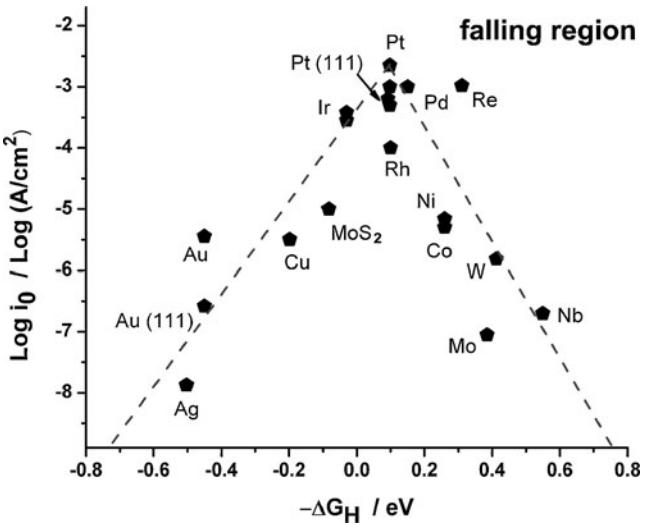

Fig. 7 Volcano plot of log i_o versus DFT-calculated Gibbs free energy of adsorbed atomic hydrogen on pure metals [94] and for nanoparticles of MoS_2 [95]. Figure adapted from [88] and [95]. Driving force increases to the right

also shows the activity of MoS_2 with experimental and theoretical data obtained by Jaramillo et al. [95]. The absolute value of the slope of both the rising and the falling branches are the same and the maximum catalytic activity is obtained for $\Delta G°_{ads}=0$. This correlation is a linear free-energy relationship since the logarithm of the reaction rate given by log i_o is directly proportional to the free energy of activation, according to transition-state theory. Many authors who have published volcano correlations like that in Fig. 7 [66] have made use of adsorption energies determined in the gas phase, so their values can differ from those that could be obtained in solution under the same conditions where the kinetic data is obtained. However, in spite of that limitation, the correlations are useful for establishing reactivity trends. A very illustrative short review on this topic has been published by Kiebler [67].

In a series of papers, Nørskov et al. [94, 96] have used ab initio methods to calculate adsorption free energies of a hydrogen atom on a series of single crystal surfaces having a face-centered cubic (111) orientation. The authors correct the calculated values for zero-point energies and for the entropy of hydrogen gas and use the value obtained to estimate the free energy of absorption of a proton in the solution phase on the metal atoms present on the electrode surface. Due to the limitations of ab initio calculations, they leave out the influence of the electric potential and field in the double-layer region and the effect of water adsorption and solvation. In spite of these limitations, Nørskov et al. have essentially corroborated the volcano correlations that have been published by other authors using experimental data only.

Recently, Schmickler and Trasatti [97] acknowledged the contributions of Nørskov et al. as very useful, although they considered their approach as oversimplistic. For example, of the metals studied, Pt is the most active catalyst. Nørskov et al. explain this by stating that, for Pt $\Delta G°_{ads}=0$ (apex of the volcano), which was pointed out by Parsons in 1958 [93]. However, experimentally, at pH=0, Pt is covered by a monolayer of H and atoms at the reversible potential for hydrogen evolution. Conway and Tilak [98] suggested in 2002 that the hydrogen involved in the HER is not this strongly adsorbed H but a weakly adsorbed species. This was confirmed later using spectroscopy [99] even though evidence for this existed in 1996 [100].

Dioxygen reduction (the oxygen reduction reaction)

At ordinary temperatures, dioxygen reduction and its anodic complement, dioxygen evolution from water, has a notoriously high overpotential, even on the most effective electrocatalysts [101]. The ground state of oxygen is a $^3P_2$ triplet, while its Group V and Group VII neighbors,

nitrogen and fluorine, are respectively a $^4S_{1.5}$ quartet and $^2P_{1.5}$ doublet. Dinitrogen is very unreactive at ordinary temperatures, while difluorine is the most reactive element. The reactivity of dioxygen falls between the two. Much of its general lack of reactivity on ordinary materials (e.g., carbon compounds) at ambient temperatures may be explained by its spin state, which also results in the molecule being paramagnetic. The result is such that its reactivity is limited by being spin-forbidden. However, at high temperatures it reacts explosively with carbon compounds and many metals in highly exothermic reactions, in which sufficient energy is released to excite it to the singlet state before reaction. At low temperatures, the normal triplet must have a suitable substrate for bonding, which limits catalysis to paramagnetic substrates, e.g., transition metals and their ligands.

As Santos and Schmickler have pointed out [70, 102], the importance of understanding the oxygen reduction reaction at low temperature is vital for the development of electrochemical energy conversion devices. They hope that the use of DFT calculations may aid this. Koper has also edited a book that addresses this subject [103]. To avoid concentration polarization problems in the electrolyte and the consequent loss of cell voltage, it is important to only use strong acid or strong alkaline electrolytes in low temperature fuel cells. Both have disadvantages: the first have inferior oxygen reduction kinetics to those in alkaline media and have a limited choice of both construction and electrocatalytic materials due to stability considerations in the medium; the second have technical problems, e.g., the well-known difficulty of carbonate formation in the electrolyte even when purified air is used and the parallel need for very pure hydrogen feedstock. Some computational approaches using DFT calculations have been made on the electrocatalysis of the ORR in acid electrolyte, but they include metals which are unstable in such media [104, 105], so their practical application is difficult to determine. In this work, Nørskov et al. [104, 105] examined the alternative rate-determining steps:

$$O_{ads} + H^+ + e^- \rightarrow OH_{ads} \tag{23}$$

$$O_{2(ads)} + H^+ + e^- \rightarrow O_2H_{ads} \tag{24}$$

They assumed that the adsorbed intermediates were identical with the species derived from water oxidation. By determination of free energies of adsorption (which are dependent on coverage), they computed the equilibrium rates as a function of these free energies using Sabatier principle analysis [71], also called Brønsted–Evans–Polanyi plot by these authors. Results show a calculated volcano plot with a rising side (positive free energy of adsorption) with a Brønsted slope of +1.67 and a falling side (lower positive free energy of adsorption to negative free energy) of −0.6 (see Fig. 8). The volcano maximum occurs at a free energy of adsorption of about +1.5 eV, where Pt (111) occurs. In conclusion, they stated that the results would be similar if second non-dissociative rds is regarded as being rate determining.

The earlier paper by Bligaard et al. quoted above [105] addresses Sabatier effects for chemical reactions involving gaseous species in which the first step is dissociative adsorption, followed by reaction with a second species to give another adsorbed intermediate, which then desorbs. In it, all adsorption phenomena are assumed to be Langmuirian. The resulting kinetic analysis is relatively complex because of the algebra involved in the dissociative reactions, but the conclusion is that a volcano will result with a rising portion as a function of more negative free energy of adsorption at high coverage of the dissociate, whose desorption is rate determining. This will be followed by a region of falling rate at low coverage, in which the dissociative chemisorption is rate determining. This corresponds to the analysis of the Volmer–Heyrovsky hydrogen evolution reaction discussed earlier, in which the adsorption is rate determining at low coverage and the desorption is rate determining at high coverage. This appears to be a general rule, provided we assume Langmuir adsorption. The Nørskov et al. paper [104] does assume that a proton is involved in the rds; however, this assumption has not been universal. The Lawrence Berkeley Laboratory workers have always maintained [3–8] that the rds of the reaction is simply $O_2 + e^- \rightarrow O_2^-$, apparently based on the fact that the overpotential for the process in acid solution is about the same as that in alkaline solution. This conclusion is meaningless since any such reaction would be expected to have no pH dependences on going from acid to alkaline solution.

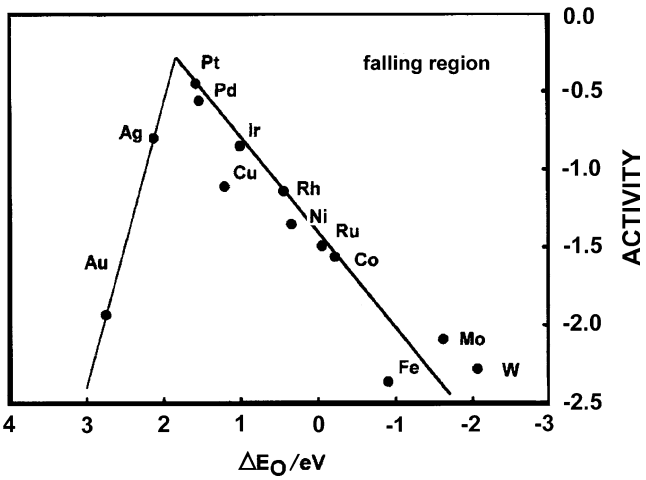

Fig. 8 Volcano plot for the reduction of O_2 plotted versus the oxygen binding energy. Adapted from Nørskov et al. [106]

Any Sabatier analysis of course does not mean that the free energy of adsorption on materials showing high coverage is the same as that on those with low coverage [9]. This would seem to be the exception rather than the rule. In general, surface repulsions will assure that the free energy of adsorption of a component will become more positive as its coverage increases. This is given by the first-order modification of the Langmuir isotherm (the Frumkin isotherm), and its simplification ignoring pre-exponential coverage terms (the Temkin isotherm; [9]). Finally, it is entirely possible that a parallel chemical process may take place around the position of maximum rate. This is alluded to by Bligaard [105], and such an effect occurs in the HOR/HER close to the equilibrium potential (the chemical Tafel reaction).

The electrochemistry of oxygen was comprehensively reviewed in 1983 [63]. Since that time, the majority of work on the ORR on Group VIII metals in acid media has been performed by workers at The Lawrence Berkeley Laboratories (to about 2003; [3–8]), with little work thereafter.

One significant piece of evidence for the problem of the rate of the ORR in acid media was been given by Will [106], who showed that for the Group 8 transition metals in 1 M $HClO_4$ the half-wave potential for dioxygen reduction at constant (room) temperature more or less coincided with the half-wave potential for reduction of the adsorbed oxygen film produced in cyclic voltammetric plots. In other words, the half-wave potential for dioxygen reduction was directly associated with that of a partial monolayer (depending on the anodic potential attained and on the time of exposure) of "oxide" (O_{ads} or OH_{ads}) reduction. The "oxide" involved in this inhibition is not the same as that involved in its initiation in a preceding anodic sweep since the anodic and cathodic waves are displaced by a cathodic potential representing a reorganization of the film, at least in the similar cases of platinum, palladium, and rhodium, in order of decreasingly negative free energy of adsorption. For these metals, the reorganized film, after an extended anodic Temkin-like adsorption isotherm, rearranges to give a Langmuir-like chemical adsorbate which desorbs as a finely marked peak so characteristic of the classical cyclic voltammetric scans on platinum. For iridium and ruthenium, the evidence is less clear, and for the first metal, in particular, the anodic and cathodic peaks (which occur at relatively cathodic potentials) are more reversible. Ruthenium behaves as an intermediate between rhodium and iridium from the viewpoint of "oxide" irreversibility, and osmium (not studied by Will) resembles it. Will and other workers provide no temperature information on the cyclic scans, which may have shed further light on the "oxide" desorption phenomena. However, indications are that it is not strongly temperature dependent. We therefore have indications of a rising volcano for dioxygen reduction, i.e., an apparent rate increase as the free energy of adsorption of OH_{ads} or O_{ads} species becomes more positive. Whether this is a Sabatier-type volcano (which is certainly the case of the Volmer–Heyrovsky mechanism for hydrogen evolution) depends on one crucial factor, which is whether the activation energy of the rising side of the volcano becomes less as the free energy of adsorption of reaction intermediates or their analogs becomes more *positive*. This was examined for dioxygen reduction on the stable elements (the platinum group metals, gold, and, marginally, silver) in concentrated orthophosphoric acid as a function of temperature in the late 1960s. Individual papers were reviewed in 1974 [42]. The first metal studied was platinum, the most active metal, which was subject to deactivation by poisoning. Later results on others became progressively more reliable as experimental difficulties in the earlier work were overcome. Results on the more strongly adsorbing metals as determined by the incipient anodic adsorption potential of OH_{ads} or O_{ads} (rhodium, iridium, ruthenium, and osmium, on the rising side of the volcano) were more stable than those on platinum and palladium, as were the results obtained on less strongly adsorbing metals (silver and gold, on the falling side). Results on osmium in particular were very stable. The activation energy for dioxygen reduction on the rising side of the volcano (osmium to platinum) *rose* in proportion to the incipient adsorption potential of OH_{ads} or O_{ads} and rose further on the descending side (silver and gold). The latter represents typical Sabatier behavior, but the rising side is atypical since it can only be explained by a *compensation effect* in which the preexponential reaction term in the Arrhenius rate expression increases to compensate for the effect of reduction in the activation energy. This had been discussed by Constable and quoted in Bond [107]. In contrast, Bligaard et al. [105] considered the preexponential term in their rate equations to be independent of the metal considered, so the rising side of the volcano was entirely dependent on decreasing activation energy. The change in preexponential factor in dioxygen reduction may be simply explained by the change in relatively temperature-independent OH_{ads} or O_{ads} adsorption on the rising side of the volcano. However, a more formal explanation is that the n_i groups of adsorption sites, each of energy E_i, are present on the surface. The total reaction rate is then $K\Sigma_0^i n_i \exp - E_{\mathrm{act},i}/RT = K'\Sigma_0^i n_i \exp - E_i/RT$ over the whole range of sites, where K, K' are constants, and $E_{\mathrm{act},i}$ is the activation energy on the E_i sites. We now suppose that n_i depends exponentially upon E_i so that $n_i = a\exp E_i/b$, where a and b are constants. The rate k_i between energies of E_i and $E_i + dE_i$ is therefore $K'\, a\exp E_i/b \exp -E_i/$

RT, and the overall rate is the sum of these over all E_i. Assuming that this is a continuous function with E_i varying from small values to some limit E, the overall rate k is:

$$k = K'a\int_0^E [(\exp E/b)(\exp - E/RT)]dE$$
$$= [K'abRT/(RT-b)][\exp E/b \exp - E/RT]dE, \text{i.e.},$$

$$\ln k = \ln[K'abRT/(RT-b)] + E/b - E/RT \quad (25)$$

Thus, the activation energy depends on the upper site energy E, and the pre-exponential term is proportional to E, in agreement with the experimental results.

This conclusion may seem to be surprising, but it can be justified as indicated below. First, for the four-electron transfer, the apparent pre-exponential term in the rate equation for the metal at the top of the volcano (platinum) and those on the falling side of the volcano (silver, gold) was about 10^5 A cm^{-2} or about 0.25 mol cm^{-2} s^{-1}. Assuming a kT/h frequency factor for a transition-state inner-sphere process, this is low and suggests that the surface coverage for the transition state itself is low, which is not a surprising conclusion. This goes a long way towards explaining why the rate of proton transfer to dioxygen on the platinum surface in the ORR is much less than that of proton transfer to platinum in the HER. In both cases, a similar "inner sphere" reorganization of H_2O from the solvated proton to ordinary water must occur. However, in the ORR case, a higher energy of activation occurs compared with that in the HER, which may imply a different surface reorganization of water molecules around, e.g., O_2H_{ads} compared with H_{ads}, if the former is the product of the ORR rds. However, it may be sufficient to explain the difference as that given by those of the enthalpies or free energies of adsorption of O_2H_{ads} and H_{ads}.

Second, we must remember that the Group VIII noble metals, starting from an essentially oxide-free surface in the underpotential hydrogen area, show in all cases adsorption of $-OH_{ads}$ and/or $-O_{ads}$ species over a wide range of potential in the form of relatively flat-topped peaks when the metals are subjected to anodic cyclic voltammetry. For some metals (Pt, Pd, Rh), surface rearrangement results in a basic single oxide phase semi-Langmuirian peak on reduction, but for the others (Ir, Ru, Os) the reduction region reflects that for adsorption.

This anodic adsorption behavior shows the presence of a variety of surface sites of different energies on these metals. It would seem that the ORR is associated with the most cathodic sites, i.e., those in the region which will be potentially free of adsorbed monolayer oxide after its reduction [107]. A study of the activation energy and the preexponential term for the ORR in other acid media would be of great value to throw light on this and to serve to give clues to how to improve the rates of the ORR, should this prove to be possible.

A recent paper reports ORR in alkaline media using Au (111), Ag(111), Pd(111), Rh(111), Ir(111), Ru(0001) single crystal surfaces and nanoparticles of the same metals [108]. It is found that the catalytic activity (as current density i) plotted versus the d-band center ($\varepsilon_d - \varepsilon_f$) gives volcano-shaped curves. $\varepsilon_d - \varepsilon_f$ is the energy of the d band relative to the energy of the Fermi level.

Linear and volcano correlations for the electrocatalytic activity of macrocyclic metal complexes incorporated on electrode surfaces

Fuel cells are clean and efficient low-emission energy-converting devices and have been known since the discovery of their principle by Grove in 1839 [109]. They have been used in space missions since the mid-1960s. However, they are still not widely used because they are expensive. There are two major drawbacks that limit their commercialization: cost and reliability. These two problems are partially linked to the slow kinetics of the oxygen cathode at close to ambient temperatures. O_2 reduction is an inner sphere reaction that involves the overall transfer of four electrons if the maximum free energy is to be released. To proceed at high rates, the ORR requires the presence of electrocatalysts as discussed in the preceding section. At present, pure platinum and (Pt)-based materials (located close or at the apex of volcano correlations) are among the major causes of limited performance and high cost of solid acid electrolyte proton exchange membrane fuel cells. Hence, many efforts have been carried over the last 40 years aimed at replacing platinum catalysts by less expensive materials. However, this goal has not been fulfilled. One approach has been to reduce the amount of Pt employed, while the other has been to investigate non-precious metal electrocatalysts of different types. Along these lines, in 1964, Jasinski [110] reported for the first time that cobalt phthalocyanine, when incorporated on a carbon support, catalyzes the reduction of O_2. This discovery triggered an intensive research in many groups around the world investigating the catalytic properties of metal phthalocyanines, metalloporphyrins, and related compounds, particularly for use in alkaline electrolytes. In general, it was found that Fe phthalocyanines catalyzed the four-electron reduction of O_2 whereas Co phthalocyanines catalyzed only the two-electron reduction, delivering almost half the free energy compared to the four-electron reduction process. These macrocyclics

have been reviewed by several authors [111–121]. In contrast to metal electrodes, electrode surfaces containing these macrocyclics present highly localized active sites (the metal centers) which are rather separated from each other by distances of at least 10 Å. In a series of seminal papers by Anson et al. [122], quoted by Zagal [117, 121], it was demonstrated that Co-cofacial–Co dinuclear porphyrins could be obtained with a Co-to-Co separation appropriate for binding oxygen on two active centers, facilitating the splitting of the O–O bond and favoring the four-electron reduction process. Later, Anson et al. [122, 123] showed that this could also be achieved by mono-nuclear Co porphyrins bearing appropriate groups on the periphery of the ligand. Mono-nuclear Fe phthalocyanines catalyze the four-electron reduction and there are still some controversies on whether they bind oxygen in such a way that the O–O bond is parallel to the phthalocyanine molecule, facilitating the splitting of the O–O bond, or that they simply catalyze the reduction of hydrogen peroxide produced from the reduction of O_2. Catalytic activity and stability can also be improved by heat treatment of these complexes combined on carbon. The amount of literature on this topic is very large and is beyond the scope of this manuscript to be discussed in any detail. As pointed out earlier, there are several reviews on this subject [111–121] so that the discussion will be focused on the establishment of free energy correlations for the catalytic activity of these compounds.

A first approach to rationalize the electrocatalytic activity of metal macrocyclics was proposed by Randin [124] in 1974 and Beck in 1977 [125] that explained the catalytic activity for O_2 reduction of phthalocyanines of different metals on the basis of a redox–catalysis process where the redox potential of the central metal ions plays a crucial role. A first theoretical explanation was provided by Ulstrup in 1977 [126]. According to Randin and Beck, during the adsorption of O_2 the metal ion in the phthalocyanine is oxidized, thereby reducing the O_2 molecule according to the scheme:

$$M(II) + O_2 \rightarrow [M(III)O_2] \tag{26}$$

$$[M(III)O_2] \rightarrow \text{products} + M(III) \tag{27}$$

In order to account for supplementary experimental evidence, a somewhat modified model was proposed by Beck [125] in which the central metal ion might also be partially oxidized. According to reactions 26 and 27 [124], the potential at which O_2 is reduced should be closely related to the M(III)/M(II) redox potential of the central metal ion. However, only in a relatively few cases have these redox potentials actually been measured in the same electrolyte in which the O_2 reduction was studied. In most cases, as reported by Randin [124], these redox potentials were measured in no aqueous solvents. The effect of pH on the redox potential is such that the water-free media is rather difficult to translate to that of the pH of water as a solvent. Moreover, the solution electrochemistry of phthalocyanines might differ from that when the complex is adsorbed or immobilized on an electrode surface. An intriguing observation by Anson et al. [127] was that, with Fe porphyrins, the onset for O_2 reduction appears at potentials well above (more positive) the Fe(III)/(II) formal potential of the adsorbed catalyst, apparently suggesting that Fe(III) was catalytic. However, Scherson et al. [128] have shown that very few Fe(II) active sites are sufficient to trigger the O_2 process and these scarcely spaced few Fe(II) sites act as highly localized nano-electrodes where rates are purely diffusion-controlled due to a very fast reaction between the Fe(II) active sites and O_2 (very fast step 26). It is important to point out here that the oxygen reduction currents are generally observed at potentials very close to the M(III)/(II) formal potential of the catalyst for Fe complexes, whereas in contrast, for Co complexes, the currents are observed at potentials far removed (more negative) than the Co(III)/(II) and this is probably due to the different O_2 binding capabilities of the two metals [113, 117, 121, 129] and to the different kinetics of step 26 for Co(II) and Fe(II).

Studies reported by van Veen et al. [120, 130] using measurements of the redox potential of the complex under the same conditions as those under which the kinetic data were obtained showed for the first time in 1979 that the activity of several metal complexes, plotted as log i at constant potential versus the M(III)/(II) redox potential of the catalyst, gave a volcano-shaped curve [130, 131]. In later papers, when studying the electrocatalytic activity of metallophthalocyanines confined on the surface of graphite electrodes, it was reported that a volcano correlation is obtained when the potential at constant current for O_2 reduction is plotted versus the M(III)/(II) redox potential of the catalyst [114]. However, later on, the same authors [132] demonstrated that the data in this figure can be better interpreted as two-linear correlations if log i at a constant potential is plotted versus the M(III)/(II) redox potential as seen in Fig. 9. One linear correlation is obtained for Cr, Mn, and Fe complexes. These metals have configurations d^4 (Cr), d^5 (Mn), and d^6 (Fe) and another linear correlation is obtained for Co complexes, which have a d^7 configuration. Shi and Zhang [129] have conducted theoretical studies that show that the ionization potential of the complexes (IP) is correlated to the redox potential of Co and Fe phthalocyanines and porphyrins. Their catalytic activity should also be correlated with IP so that plots of log k versus IP also give linear correlations. The lines in Fig. 9 are parallel with a slope close to 0.15 V/decade. The line in Fig. 9 (right) has a slope of 1.25 eV/decade and 1.1 eV/decade, demonstrating

that IP is a good reactivity index for these Co and Fe phthalocyanines and also for TPyr3,4FePz. It is possible that the declining straight lines are part of an incomplete volcano correlation. If so, the slope $(\delta E^{\circ\prime}/\delta \log i)_E$ of 0.15 V/decade might have a physical meaning, as it was discussed for the oxidation of thiols [121, 132]. So, using similar arguments to those discussed for the oxidation of thiols, the slope of 0.15 V/decade would correspond to the falling region of an incomplete volcano. For the data in Fig. 9, the driving force of the catalyst increases as the formal potential of the catalysts becomes more negative. Hence, if $\Delta G_{\mathrm{adsO2}}$ is the free energy of step 18, then the more negative the formal potential of the catalyst the more negative $\Delta G_{\mathrm{ads\ O2}}$ Hence, the rate of the falling region of the volcano would be:

$$v = C\exp + [\beta' \Delta G_{\mathrm{adsO_2}}/RT] \exp -[\beta E F/RT] \tag{28}$$

and since kinetic data are compared at constant E, the second exponential term is constant so that Eq. 28 can be rewritten as:

$$v = C'\exp + [\beta' \Delta G_{\mathrm{adsO_2}}/RT] \tag{29}$$

$$\text{so assuming that } \Delta G_{\mathrm{adsO_2}} \approx nFE^{\circ\prime} + C'' \tag{30}$$

$$v = C'''\exp + [\beta' E^{\circ\prime}/RT] \tag{31}$$

where C''' contains the constant exponential terms.

Equation 31 predicts a slope $(\delta \log i/\delta E^{\circ\prime})_E$ of the plot of log v versus $E^{\circ\prime}$ of $2.303RT/\beta'$, which for values of $\beta'=0.5$ gives a slope of 0.118 V/decade. This is not far from the experimental values. These results indicate that $\Delta G_{\mathrm{adsO_2}}$ is probably linked to the M(III)/(II) formal potential of the catalysts as pointed out earlier by Randin and Beck since the interaction of the dioxygen molecule with the active site involves the partial oxidation of the metal center. Further, Shi and Zhang [129] have found that, in the plots of Fig. 9, the energy of interaction of the metal center in Co complexes with the O_2 molecule increases from left to right so that might be a further indication that the straight lines in Fig. 9 correspond to the falling side of a volcano.

The data in Fig. 9 indicate that more positive redox potentials will increase the catalytic activity up to a certain point if the correlation is an "incomplete volcano". The M (III)/M(II) redox potential of some macrocyclics can be shifted in the positive direction with heat treatment. For example, when iron tetraphenyl porphyrin [133], 4(Ph)FeP, is heat-treated, the Fe(III)/(II) redox transition is shifted from 0.2 V vs RHE for fresh 4(Ph)FeP to 0.4 V for 4(Ph)FeP heat-treated at 700 °C. Intermediate redox potentials are obtained for heat treatments at intermediate temperatures [133] and the catalytic activity increases with heat treatment, showing that a more positive redox potential of the catalyst favors the O_2 reduction reaction rate.

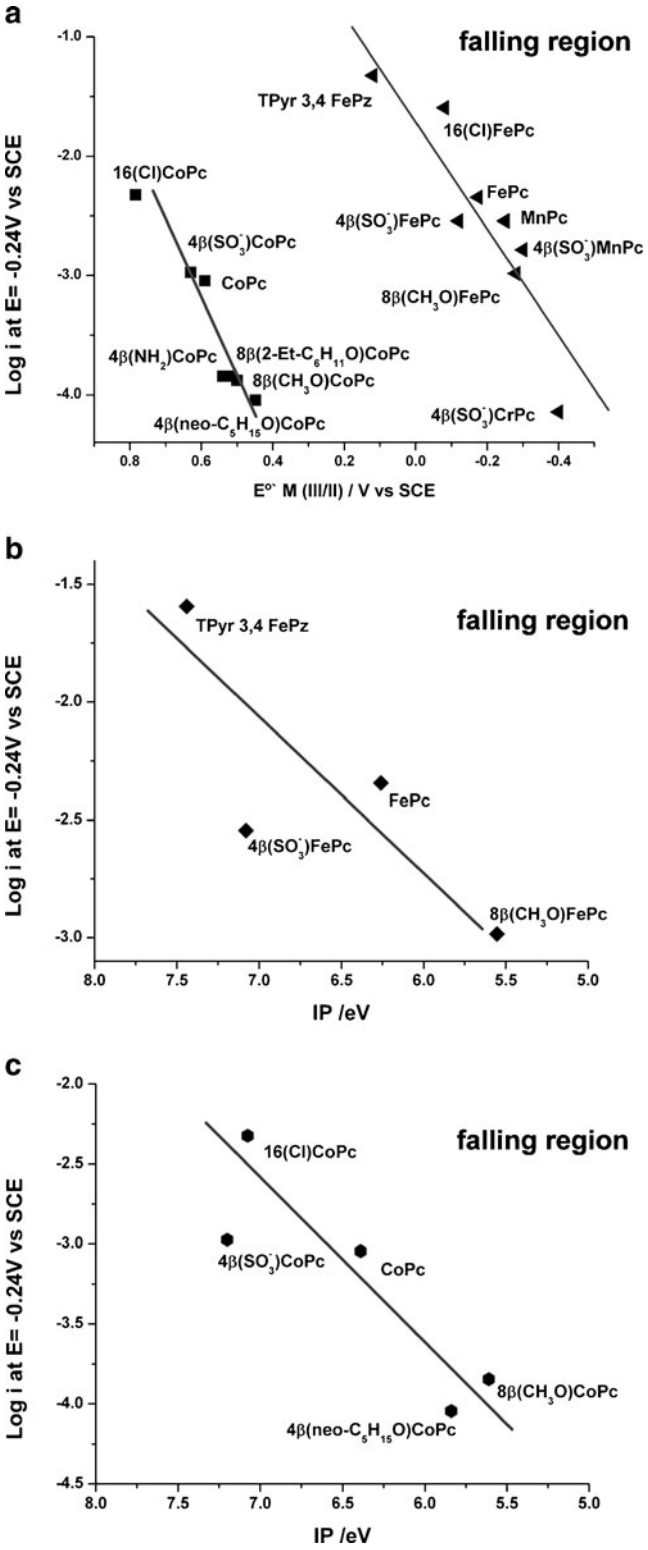

Fig. 9 **a**–**c** Plots of log I at constant E versus the formal potential of the catalyst (*left*) an similar plot versus the calculated ionization potential of the catalyst. Reduction of O_2 in 0.1 M NaOH. Adapted from Fig. 14 in [137]

It has been found over the years [113, 115, 117, 132, 134, 136–138], when studying the electrocatalytic activity of surface-confined macrocyclic complexes for many other reactions other than O_2 reduction (oxidation of several thiols, glucose, thiocyanate, hydrazine), that volcano plots are obtained when log i at constant E is compared versus the formal potential $E^{\circ\prime}$ of the catalyst. The slope of the rising portion $(\delta E^{\circ\prime}/\mathrm{dlog}i)_E$ is close to +0.120 V/decade and it is identical to the Tafel slope $(\delta E/\mathrm{dlog}i)_{E^{o\prime}}$ obtained from plots constructed with kinetic data for the oxidation of a given thiol on an electrode modified with a single Co catalyst. This is also true when complexes of different metals are studied [121, 132, 134, 136–138]. This is true for many other reactions [121], which shows that the formal potential of the catalyst is the driving force of the reaction at constant electrode potential, in an analogous way of a Tafel plot of log i versus E at constant $E^{\circ\prime}$ (using a single catalyst). A mathematical expression for both branches of the volcano plots is discussed later, showing that for some reactions these correlations are symmetrical whereas for other reactions, involving ionic species, they are not. These correlations show that the formal potential of the catalyst is related to the free energy of adsorption of the reacting molecule on the active sites (metal centers on the surface confined complexes).

The derivation below explains the volcano correlation of Fig. 10 using a Langmuir isotherm for the adsorbed target molecule (thiocyanate, thiolate, hydrazine, etc.; [121, 134, 136–138]) whose solution activity is $a_{\mathrm{SCN}^-\mathrm{sol}}$ and whose free energy of adsorption is $\Delta G_{\mathrm{SCN}^-}$:

$$\theta = a_{\mathrm{SCN}^-\mathrm{sol}}\exp(-\Delta G_{SCN} - /RT)/ [1 + a_{\mathrm{SCN}^-\mathrm{sol}}\exp(-\Delta G_{\mathrm{SCN}} - /RT)] \quad (32)$$

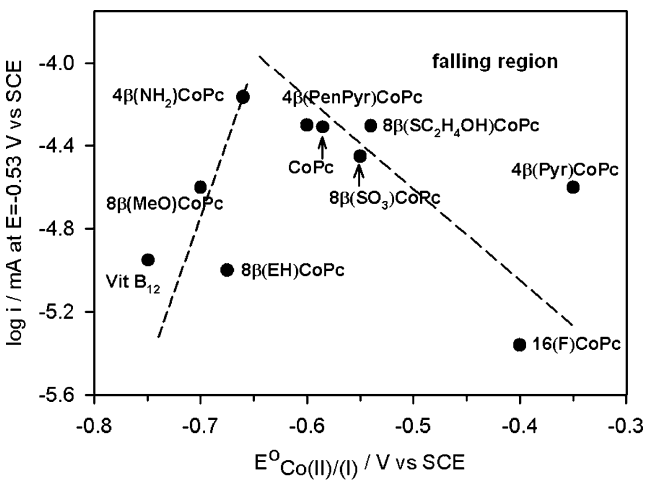

Fig. 10 Volcano plot for the oxidation of thiocyanate at pH 4, catalyzed by surface-confined Co macrocyclics. Reproduced with permission from Wiley; Fig. 4 of [138]

The rate of the reaction for a given applied potential E is

$$v = \theta C\exp + [(1-\beta')\Delta G_{\mathrm{SCN}} - /RT]\exp + [(1-\beta)EF/RT] \quad (33)$$

$$v = a_{\mathrm{SCN}^-\mathrm{sol}}C\exp - [\beta'\Delta G_{SCN} - /RT]\exp + [(1-\beta)EF/RT]/[1 + a_{\mathrm{SCN}^-\mathrm{sol}}\exp(-\Delta G_{SCN} - /RT)] \quad (34)$$

Essentially, θ can vary between 0 and 1. For very small values of θ, $\Delta G_{\mathrm{SCN}^-}$ is very positive and Eq. 34 becomes:

$$v = a_{\mathrm{SCN}^-\mathrm{sol}}C\exp - [\beta'\Delta G_{\mathrm{SCN}} - /RT]\exp + [(1-\beta)EF/RT \quad (35)$$

For gradually more negative values of $\Delta G_{\mathrm{SCN}^-}$, $\theta \rightarrow 1$ and Eq. 34 become:

$$v = C\exp + [(1-\beta')\Delta G_{\mathrm{SCN}} - /RT]\exp + [(1-\beta)EF/RT] \quad (36)$$

If one compares the catalytic activities of different complexes at an arbitrary fixed potential, then Eqs. 35 and 36 become:

$$v = a_{\mathrm{SCN}^-\mathrm{sol}}C'\exp[-\beta'\Delta G_{\mathrm{SCN}} - /RT]\text{for low } \theta \quad (37)$$

$$v = C'\exp[+(1-\beta')\Delta G_{\mathrm{SCN}} - /RT]\text{for high } \theta \quad (38)$$

Equations 37 and 38 explain the rising and falling regions in the volcano correlation and suggest that the formal potential of the catalyst is proportional to ΔG of adsorption of the target molecule. Experimentally, the slope of the falling region is found to be larger than that predicted by Eq. (38), but this seems to be true only for charged species [121, 134, 136–138]. For O_2 reduction (Fig. 8) and for the oxidation of hydrazine, the slope of the falling region is close to $-RT/\beta'F$ [121]. This can be attributed to the fact that, when charged species are involved, a correction must be introduced in the exponential terms $\Delta G_{\mathrm{SCN}^-}$, as discussed in [137].

Conclusions

Free energy correlations are the essence of electrode kinetics and they were established long ago by the empirical Tafel equation and then by the Butler–Volmer equation that is supported by the transition state theory. The Tafel equation predicts a linear correlation between log i

and the overpotential, with a slope of $RT/\alpha F$. It is interesting to point out that Tafel established his famous equation using the HER and not a simple outer-sphere redox process like $Fe^{3+}_{(aq)} + e \leftrightarrows Fe^{2+}_{(aq)}$, for example. HER in aqueous media is an inner-sphere rather complicated reaction, as discussed in this article. Both Butler–Volmer [39] and Tafel equations [60] can be derived from first principles. However, the transfer coefficient α may depend on temperature and also on the overpotential. Reactions taking place in the solution phase that undergo a redox catalytic process may proceed via an outer-sphere mechanism, and the driving force of the reaction is given by the redox potential of the catalyst. This is very relevant to organic electrochemistry. The electrode potential is not the driving force of the reaction since a direct reaction between the electrode and the reacting molecule does not take place. The electrode only participates in regenerating the active form of the catalyst. Interestingly, a plot of log k versus the redox potential of the catalyst gives a linear correlation with a slope similar to a Tafel slope, with a value close to 0.118 V/decade.

However, when the electrode surface participates in the reaction as a catalyst, reaction rates and/or i_o values are strongly dependent on the nature of electrode material. Well-studied reactions such as the HER, which is a venerable topic in electrochemistry and has generated a myriad of publications, are still the subject of intensive research, with the aim of understanding the fundamentals of the electrocatalytic process. In spite of its apparent simplicity, there are still features which are difficult to model theoretically. Correlations between catalytic activity (as log i_o) versus the free energy of adsorption of hydrogen atoms on the catalytic surface give the well-known volcano correlations. The rising portion of the volcano resembles a Tafel plot since log i_o increases linearly with the driving force of the reaction, so the slope should be $RT/\beta' F$ which is similar to a Tafel slope of $RT/\beta F$. The falling region of the volcano correlation, strictly speaking, is not a free energy correlation because the change in the sign of the slope is due to a gradual decrease in the number of free active sites and not to activation-related phenomena.

In the case of electrodes modified with metal complexes, the same logics apply. In these, free energies of adsorption of reactant with the metal centers in the complex catalysts are related to the redox potential (M(III)/(II) or M(II)/(I)) depending on the reaction. Symmetrical and asymmetrical volcano correlations are obtained for several reactions but, for all cases, the slope of the raising region of the volcano is close to $RT/\beta' F$, indicating that if activities are compared at constant potential, the redox potential acts as the driving force of the reaction.

A general conclusion from electrocatalytic phenomena is that if volcano correlations are well established, then for a particular reaction the properties of the catalyst can be "tuned" so as to improve their activity. The optimal properties can involve many other parameters such as metal-to-metal separation, crystal orientation, stability, alloying, nanostructure, and redox potential of catalyst, so this is an open field for both experimentalists and theoreticians to find ways of improving the catalytic activity of electrode surfaces. The implications of future development in this area will have a tremendous impact in energy conversion devices, electrosynthesis, electrochemical sensors, and bioelectrochemistry just to mention a few.

Finally, we want to point out to that this volume includes an article by G. Inzelt describing the milestones in the development of electrode kinetics that can be very useful to the reader and includes photographs of Tafel, Butler, Erdey-Gruz, Volmer, Frumkin, Polányi, and Marcus [138].

Acknowledgements This work has been financed by Fondecyt Project 1100773, Núcleo Milenio de Ingeniería Molecular P07-006. The authors are grateful to editors F. Scholz, S. Fletcher, and G. Inzelt for their helpful suggestions and to J.F. Silva for useful comments.

References

1. Frumkin AN (1932) Z Phys Chem Leipz 160:120
2. Bockris JOM, Khan SUM (1993) Surface electrochemistry, a molecular level approach. Plenum, New York
3. Marković NM, Ross PN (2002) Surf Sci Rep 45:117
4. Markovic NM, Ross PN (1999) Electrocatalysis at well-defined surfaces: kinetics of oxygen reduction and hydrogen oxidation/evolution on Pt(*hkl*) electrodes. In: Wieckowski A (ed) Interfacial electrochemistry: theory, experiment, and applications. Marcel Dekker, New York, pp 821–841
5. Schmidt TJ, Stamenkovic V, Arenz M, Markovic NM, Ross PN (2002) Electrochim Acta 47:3765
6. Blizanac BB, Stamenkovic V, Marković NM (2007) Z Phys Chem 221:1379
7. Stamenkovic VR, Mun BS, Arenz M, Mayrhofer KJJ, Lucas CA, Wang G-F, Ross PN, Marković NM (2007) Nat Mater 6:241
8. Stamenkovic VR, Fowler B, Mun BS, Wang G, Ross PN, Lucas CA, Marković NM (2007) Science 315:493
9. Damjanovic A, Brusic V (1967) Electrochim Acta 12:615
10. Schrödinger E (1926) Phys Rev 28:1049
11. Gurney RW (1931) Proc Roy Soc A134:137
12. Marcus RA (1956) J Chem Phys 24:966
13. Conway BE (1964) Proton solvation and proton transfer processes in solution. In: Bockris JOM, Conway BE (eds) Modern aspects of electrochemistry, vol 3. Butterworth, London, pp 43–148
14. Appleby AJ (2005) Electron transfer reactions with and without ion transfer. In: Bockris JOM, Conway BE, Vayenas CG, White RE, Gamboa-Adelco ME (eds) Modern aspects of electrochemistry, vol 38. Kluwer, New York, pp 175–301
15. Marcus RA (1957) J Chem Phys 26:867
16. Marcus RA (1963) J Chem Phys 38:1858
17. Marcus RA (1963) 39:1734
18. Franck J (1926) Trans Faraday Soc 21:536
19. Franck J (1926) Z Phys Chem 120:144
20. Condon EU (1926) Phys Rev 28:1182
21. Condon EU (1928) Phys Rev 32:858

22. Born M, Oppenheimer R (1927) Annal Phys 84:457
23. Marcus RA (1960) Disc Faraday Soc 29:21
24. Marcus RA (1963) J Phys Chem 67:853, 2889
25. Marcus RA (1965) J Chem Phys 43:679
26. Marcus RA (1968) J Phys Chem 72:891
27. Marcus RA, Cohen A (1968) J Phys Chem 72:4249
28. Johnston HS (1960) Adv Chem Phys 3:131
29. Hush NS (1957) Z Elektrochem 61:734
30. Hush NS (1958) J Chem Phys 28:962
31. Hush NS (1961) Trans Faraday Soc 57:557
32. Levich VG (1966) Present state of the theory of oxidation–reduction in solution (bulk and electrode reactions). In: Delahay P (ed) Advances in electrochemistry and electrochemical engineering, vol 4. Interscience, New York, pp 249–371
33. Levich VG, Eyring HD, Henderson D, Jost Y, Levich VG (1970) Kinetics of reactions with charge transport. In: Eyring HD, Henderson D, Jost Y (eds) Physical chemistry, vol 9B. Academic, New York, pp 985–1074
34. Dogonadze RR (1972) Theory of molecular electrode kinetics. In: Hush NS (ed) Reactions of molecules at electrodes. Wiley, New York, pp 135–227
35. Appleby AJ, Bockris JO'M, Sen RK, Conway BE (1972) Quantum mechanics of charge transfer at interfaces. In: Buckingham AD, Bockris JO'M (eds) MTP Int Rev Sci Phys Chem Ser 1, vol 6. Butterworth, London, pp 1–40
36. Dogonadze RR, Kuznetsov AM, Levich VG (1968) Electrochim Acta 13:1095
37. Dogonadze RR, Kuznetsov AM (1983) Quantum electrochemical kinetics: continuum theory. In: Conway BE, Bockris JO'M, Yeager E, Khan SUM, White RE (eds) Comprehensive treatise on electrochemistry. Plenum, New York, pp 1–40
38. Bernal JD, Fowler RH (1933) J Chem Phys 1:515
39. Koper MTM, Schmickler W (1998) A unified model for electron and ion transfer reactions on metal electrodes. In: Lipkowski J, Ross PN (eds) Electrocatalysis. Wiley, New York, pp 291–322
40. Laidler KJ, Sacher E (1964) Theories of elementary electron transfer reactions. In: Bockris JO'M, Conway BE (eds) Modern aspects of electrochemistry, vol 3. Butterworth, London, pp 1–42
41. Conway BE, Bockris JO'M (1961) Electrochim Acta 3:340
42. Appleby AJ (1974) Electrocatalysis. In: Bockris BE, Conway BE (eds) Modern aspects of electrochemistry, vol 3. Butterworth, London, pp 369–478
43. Booth F (1951) J Chem Phys 19:391
44. Khan SUM, Bockris JO'M (1983) Molecular aspects of quantum electrode kinetics. In: Conway BE, Bockris JO'M, Yeager E, Khan SUM, White RE (eds) Comprehensive treatise on electrochemistry. Plenum, New York, pp 41–86
45. Krishtalik LI (1957) Zh Fiz Khim 31:33
46. Miller JR, Calcaterra LT, Closs GL (1984) J Am Chem Soc 106:3047
47. Kadhum AAH, Salmon GA (1982) Faraday Disc Chem Soc 74:191
48. Chidsey CED (1991) Science 251:919
49. Nahir TM, Clark RA, Bowden EF (1994) Anal Chem 66:2595
50. McLendon G, Hake R (1992) Chem Revs 92:481
51. Zhang J, Kuznetsov AM, Medvedev IG, Chi Q, Albrecht T, Jensen PS, Ulstrup J (2008) Chem Revs 108:2737
52. McLendon G (1988) Acc Chem Res 21:160
53. Kakitani T, Matanaga N (1985) J Phys Chem 89:8
54. Fletcher S (2007) J Solid State Electrochem 11:965
55. Fletcher S (2008) J Solid State Electrochem 12:765
56. Fletcher S (2008) J Solid State Electrochem 12:1511
57. Tafel J (1905) Z Phys Chem 50:641
58. Petrii OA, Nazmutdinov RR, Bronshtein MD, Tsirlina GA (2007) Electrochim Acta 52:3493
59. Hupp J, Ram MS (1990) J Phys Chem 94:2378
60. Fletcher SJ (2009) Solid State Electrochem 13:537
61. Parsons P, quoted by Hoar TP (1956) in Proc 8th Meeting C.I.T. CE., Madrid, Butterworth, London p 439
62. Schmickler W, Santos E (2010) Interfacial Electrochemistry, 2nd edn. Springer, Heidelberg
63. Conway BE, Bockris JO'M, Yeager E, Khan SUM, White RE (eds) (1983) Comprehensive treatise of electrochemistry. Plenum, New York
64. Santos E, Lundin A, Pöttin K, Quaino P, Schmickler W (2009) J Solid State Electrochem 13:1101
65. Calvo E (2002) Fundamentals. The current–potential relationship. In: Bard AJ, Stratmann M, Gileadi E, Urbakh M (eds) Encyclopedia of electrochemistry, thermodynamics and electrified interfaces. 1:3 Wiley, pp 3–30
66. Conway BE (1965) Theory and principles of electrode processes. Ronald, New York
67. Kiebler LA (2006) Chem Phys Chem 7:98
68. Bockris JO'M, Mauser H (1959) Can J Chem 37:475
69. Appleby AJ (1983) Electrocatalysis. In: Conway BE, Bockris JO'M, Yeager E, Khan SUM, White RE (eds) Comprehensive treatise of electrochemistry, vol 2. Plenum, New York, pp 173–239
70. Santos E, Schmickler W (2010) Recent advances in theoretical aspects of electrocatalysis. In: Balbuena P, Subramanian V (eds) Theory and experiment in electrocatalysis. Modern aspects of electrochemistry, vol 50. Springer, New York, pp 25–70
71. Sabatier P (1911) Ber Deutsch Chem Gesell 44:1984
72. Lexa D, Mispelter J, Savéant JM (1981) J Am Chem Soc 103:6806
73. Lexa D, Savéant JM, Wang DL (1986) Organometalics 5:1428
74. Lexa D, Savéant JM, Su K-B, Wang DL (1987) J Am Chem Soc 109:6464
75. Lexa D, Savéant JM, Schäfter HJ, Su K-B, Vering B, Wang DL (1990) J Am Chem Soc 112:6162
76. Savéant JM (2006) Elements of molecular and biomolecular electrochemistry. Wiley, Hoboken, pp 251–296
77. Astruc D (1995) Electron transfer and radical processes in transition-metal chemistry. VHC Publishers Inc, New York
78. Savéant JM (1987) J Am Chem Soc 109:6788
79. Savéant JM (1993) Acc Chem Res 26:455
80. German ED, Kuznetsov AM (1994) J Phys Chem 98:6120
81. Workentin MS, Maran F, Wayner DDM (1995) J Am Chem Soc 117:2120
82. Donker RL, Maran F, Wayner DDM, Workentin MS (1999) J Am Chem Soc 121:7248
83. Maran F, Wayner DDM, Workentin MS (2001) Adv Phys Org Chem 36:85
84. Santos E, Koper MTM, Schmickler W (2008) Chem Phys 344:195
85. Koper MTM, Voth GA (1998) Phys Lett 282:100
86. Calhoun A, Koper MTM, Voth GA (1999) J Phys Chem B 103:3442
87. Kobosev N, Monblanova W (1934) Acta Physicochim URSS 1:611
88. Kobosev N, Monblanova W (1936) Acta Physicochim URSS 4:395
89. Horiuti J, Polanyi M (1935) Acta Physochim URSS 2:50
90. Trasatti S (1972) J Electroanal Chem 39:163
91. Trasatti S (1994) Electrochim Acta 39:1803
92. Gerischer H (1958) Bull Soc Chim Belg 67:506
93. Parsons R (1958) Trans Faraday Soc 54:1053
94. Nørskov JK, Bligaard T, Logadottir A, Kitchin JR, Chen JG, Pandelov S, Stimming U (2005) J Electrochem Soc 152:J23
95. Jaramillo TF, Jørgensen KP, Bonde J, Nielsen JH, Horch S, Chorkendorff I (2007) Science 317:100
96. Meier J, Schløtz J, Liu P, Nørskov JK, Stimming U (2004) Chem Phys Lett 390:440

97. Schmickler W, Trasatti S (2006) J Electrochem Soc 153:L31
98. Conway BE, Tilak BV (2002) Electrochim Acta 47:3371
99. Kunimatsu K, Uchida H, Osawa M, Watanabe M (2006) J Electroanal Chem 587:209
100. Tadjeddine A, Peremans A (1996) J Electroanal Chem 409:115
101. Appleby AJ (1993) J Electroanal Chem 357:117
102. Santos E, Schmickler W (eds) (2011) Catalysis in electrochemistry: from fundamental aspects to strategies for fuel cell development. Wiley, New York
103. Koper M (ed) (2009) Fuel cell catalysis: a surface science approach. Wiley, New York
104. Nørskov JK, Rossmeisl J, Logadottir A, Lundquist L, JKitchim JR, Bligaard T, Jónsson H (2004) J Phys Chem B 108:17886
105. Bligaard T, Nørskov JK, Dahl S, Matthiesen J, Christensen CH, Sebested J (2004) J Catal 224:206
106. Will F (1975) The role of oxides in the electroreduction of oxygen. In: Conference proceedings, Fuel Cell Catalysis Workshop, special report, EPRI SR-13. Electric Power Research Institute, Palo Alto, CA, pp 71–76
107. Bond GC (1962) Catalysis by metals. Academic, New York
108. Lima FHB, Zhang J, Shao MH, Sasaki K, Vukmirovic MB, Ticianelly EA, Adzic RR (2007) J Phys Chem C 111:404
109. Grove WR (1839) Phil Mag 14:127
110. Jasinski R (1964) Nature 201:1212
111. van den Brink F, Barendrecht E, Visscher W (1980) Rec J R Neth Chem Soc 99:253
112. Tarasevich MR, Radiushkina KA (1980) Russ Chem Ver 49:718
113. Zagal JH (1992) Coord Chem Rev 119:89
114. Adzic RR (1998) Recent advances in oxygen reduction. In: Lipkowski J, Ross PN (eds) Electrocatalysis. Wiley, New York, pp 291–242
115. Zagal JH (2003) Macrocycles. In: Vielstich W, Lamm A, Gasteiger H (eds) Handbook of fuel-cell. Fundamentals, technology and applications, vol 2, part 5. Wiley, Chichester, pp 544–554
116. Dodelet JP (2006) Oxygen-reduction in PEM fuel-cell conditions: heat-treated non-precious metal-N4 macrocycles and beyond. In: Zagal JH, Bedioui F, Dodelet JP (eds) N4 macrocyclic metal complexes. Springer, New York, pp 83–147
117. Zagal JH, Paez MA, Silva JF (2006) Fundamental aspects of the catalytic activity of metallomacrocyclics for the reduction of O_2. In: Zagal JH, Bedioui F, Dodelet JP (eds) N4 macrocyclic metal complexes. Springer, New York, pp 41–75
118. Bezerra CWB, Zhang L, Liu H, Lee K, Marques ALB, Marques EP, Wang H, Zhang J (2007) J Power Sources 173:891
119. Zhang L, Zhang J, Wilkinson DP, Wang H (2006) J Power Sources 156:171
120. Song C, Zhang J (2008) PEM fuel cell electrocatalysts and catalyst layers. In: Zhang J (ed) Fundamentals and applications. Springer, New York, p 89
121. Zagal JH, Griveau S, Silva JF, Nyokong T, Bedioui F (2011) Coord Chem Rev 254:2755
122. Collman JP, Denisevich P, Konai Y, Marrocco M, Koval C, Anson FC (1980) J Am Chem Soc 102:607
123. Steiger B, Shi C, Anson FA (1993) Inorg Chem 32:2107
124. Randin JP (1974) Electrochim Acta 19:83
125. Beck F (1977) J Appl Electrochem 7:191
126. Ulstrup (1977) J Electroanal Chem 79:191
127. Shigehara K, Anson F (1982) J Phys Chem 86:2776
128. Zhu H, Tolmachev YV, Scherson DA (2010) J Phys Chem C 114:13650
129. Shi Z, Zhang J (2007) J Phys Chem C 111:7084
130. Van Veen JAR, Visser C (1979) Electrochim Acta 24:921
131. Van Veen JAR, Van Baar JF, Kroese CJ, Coolegem JGF, De Wit N, Colljn HA (1981) Ber Bunsenges Phys Chem 85:693
132. Zagal JH, Gulppi M, Isaacs M, Cárdenas-Jirón G, Aguirre MJ (1998) Electrochim Acta 44:1349
133. Bouwkamp-Wijnoltz AL, Visscher W, Van Veen JAR, Boellard E, Van der Kraan AM, Tang SC (2002) J Phys Chem B 106:12993
134. Zagal JH, Gulppi MA, Caro CA, Cárdenas-Jirón GI (1999) Electrochem Comm 1:389–393
135. Cárdenas-Jirón GI, Gulppi MA, Caro CA, Del Río R, Páez M, Zagal JH (2001) Electrochim Acta 46:3227
136. Bedioui F, Griveau S, Nyokong T, Appleby AJ, Caro CA, Gulppi M, Ochoa G, Zagal JH (2007) Phys Chem Chem Phys 9:3383
137. Sancy M, Pavez J, Gulppi MA, Mattos IL, Arratia-Perez R, Linares-Flores C, Páez M, Nyokong T, Zagal JH (2011) Electroanalysis 23:711
138. Inzelt G (2011) J Solid State Electrochem (in press)